POLITECNICO DI TORINO
Repository ISTITUZIONALE

3D Cell Culture: Recent Development in Materials with Tunable Stiffness

Original
3D Cell Culture: Recent Development in Materials with Tunable Stiffness / Baruffaldi, D., Palmara, G., Pirri, C., Frascella, F.. - In: ACS APPLIED BIO MATERIALS. - ISSN 2576-6422. - ELETTRONICO. - 4:3(2021), pp. 2233-2250. [10.1021/acsabm.0c01472]

Availability:
This version is available at: 11583/2922716 since: 2021-09-09T17:38:31Z

Publisher:
American Chemical Society

Published
DOI:10.1021/acsabm.0c01472

Terms of use:

This article is made available under terms and conditions as specified in the corresponding bibliographic description in the repository

Publisher copyright

(Article begins on next page)

12 September 2026

ACS APPLIED BIO MATERIALS

www.acsabm.org Review

3D Cell Culture: Recent Development in Materials with Tunable Stiffness

Désirée Baruffaldi, Gianluca Palmara, Candido Pirri, and Francesca Frascella*

Cite This: *ACS Appl. Bio Mater.* 2021, 4, 2233–2250 Read Online

ACCESS | Metrics & More | Article Recommendations

ABSTRACT: It is widely accepted that three-dimensional cell culture systems simulate physiological conditions better than traditional 2D systems. Although extracellular matrix components strongly modulate cell behavior, several studies underlined the importance of mechanosensing in the control of different cell functions such as growth, proliferation, differentiation, and migration. Human tissues are characterized by different degrees of stiffness, and various pathologies (e.g., tumor or fibrosis) cause changes in the mechanical properties through the alteration of the extracellular matrix structure. Additionally, these modifications have an impact on disease progression and on therapy response. Hence, the development of platforms whose stiffness could be modulated may improve our knowledge of cell behavior under different mechanical stress stimuli. In this review, we have analyzed the mechanical diversity of healthy and diseased tissues, and we have summarized recently developed materials with a wide range of stiffness.

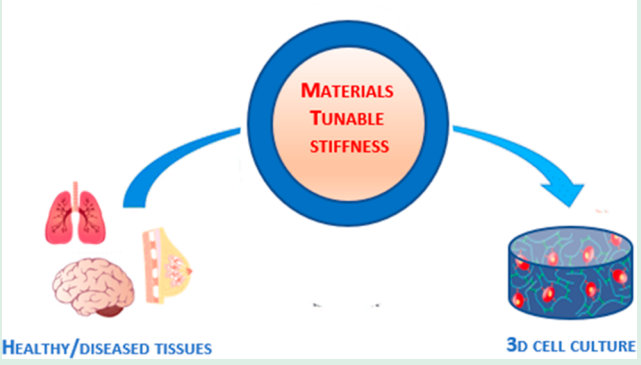

KEYWORDS: *3D cell culture, stiffness, mechanical properties, tissue mimic, tunable materials, hydrogels*

Downloaded via 151.46.95.43 on September 10, 2021 at 16:21:54 (UTC).
See https://pubs.acs.org/sharingguidelines for options on how to legitimately share published articles.

1. INTRODUCTION

Until about 20 years ago, the earliest attempts to grow cells in three dimensions (3D) showed great promise as this culturing method allowed scientists to better mimic the anatomical structures that are present in the human body. However, very few laboratories had successfully set up to develop 3D techniques. Cells cultured on 3D matrices behave in a dissimilar way compared to the traditional 2D culture systems, as the latter method shows a strong limitation in the lack of all the complex interactions that occur in the tissue microenvironment, affecting cell morphology, growth, and drug response.[1] Moreover, gene expression analyses identified significant inconsistencies between cells grown as a monolayer or as 3D cultures, with the latter being capable of inducing the same expression levels found in vivo.[2,3] For instance, cells of glioblastoma multiform (GBM) showed differential expression in genes involved in cell and cell−cell adhesion, chemokine and cytokine signaling, nervous system development, and focal adhesion pathways when cultured in 3D scaffolds compared to 2D monolayers.[4] Importantly, studies on cancer cell features took advantage of 3D culture; it is well-known that the tumor microenvironment consists of several cell types, matrix components, and signaling molecules.[5] 2D culture systems failed in reproducing this complex compartment; instead, 3D platforms allowed to preserve the shape, polarization, genetic profile and heterogeneity of cancer cells and the stroma.[6] Furthermore, the microenvironment is responsible for modulating the response to anticancer drugs through the vasculature architecture, acidic tumor environment, presence of hypoxic regions, and interactions between tumor and stromal cells.[7] Studies carried out on glioblastoma cells revealed that cells cultured in scaffolds responded differently to therapeutic agents, and 3D models could represent a helpful tool for testing drug efficacy.[8−10]

The mechanical properties of the extracellular matrix (ECM) have a significant impact on a wide range of cell behaviors such as growth, differentiation, adhesion, and signal transduction. Cells are indeed able to perceive external mechanical stimuli and activate molecular pathways related to mechanotransduction in response; the magnitude, the spatial orientation, and the time course of these mechanical stimuli influence the type and the strength of the response. Hence, the stiffness of the extracellular environment regulates

Received: November 11, 2020
Accepted: February 19, 2021
Published: February 26, 2021

ACS Publications

© 2021 The Authors. Published by American Chemical Society

https://dx.doi.org/10.1021/acsabm.0c01472
ACS Appl. Bio Mater. 2021, 4, 2233−2250

cytoskeletal structure and cell-matrix protein organization, which are linked to important processes such as cell division, migration, and apoptosis.[11] As well depicted in the review of Kechagia and colleagues, integrins on cell membranes act as sensors of mechanical signals derived from ECM. Specifically, they could form multiprotein plaques in response to an elastic strain leading to cytoskeletal rearrangement, gene transcription, and activation of signaling proteins. Integrins are fundamental also in durotaxis which is the cell migration guided by ECM rigidity.[12] Moreover, Nemec and colleagues underlined how matrix stiffness could influence chromatin architecture and epigenetic signature. For example, the translocation into the nucleus of transcriptional regulators YAP (Yes-associated protein) and TAZ (PTZ-binding motif) after matrix stiffening has been seen to cause chromatin modification.[13] Additionally, metabolism is modulated by changes in ECM mechanical properties. Indeed, softening seems to be correlated to reduce glycolysis because of the inhibition of enzymes involved in the process. Contrariwise, YAP-TAZ translocation promotes glycolysis and autophagy, thus increasing cell proliferation in stiffer matrix.[14] 3D models and the modulation of their stiffness enable the study of external stimuli effects on cells *in vitro* and represent a valuable tool for mimicking both physiological and pathological conditions.[15−18] As shown in Figure 1, tissues were

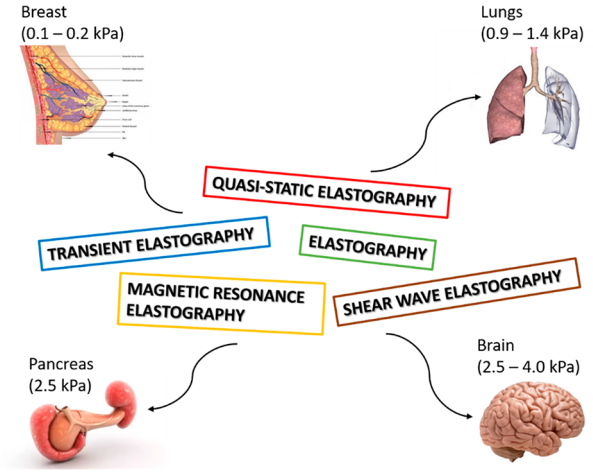

Figure 1. Picture summarizing stiffness values of the main human tissues in a healthy condition. The fibrotic tissues become stiffer than those in normal conditions. In the middle, an overview of several techniques, based on elastography, used to measure tissue stiffness.

characterized by a specific range of stiffness because of their composition, heterogeneity, and position. These conditions were perturbed during disease progression, leading to a more aggressive or debilitating prognosis.[19−21] In recent years, attention has been increasingly attracted by the micropatterning of soft material surfaces. In this way, the materials tend to mimic natural morphologies on the micro/nanometer scale.[22,23] There were numerous studies investigating the theme of 3D patterning approaches in soft materials including self-rolling,[24,25] origami-inspired,[26,27] and 3D or 4D printing.[28−30] The latter has become the last frontier and consists in biomaterials also called intelligent materials, that have, as an additional feature, the sensitivity to external stimuli. In fact, 4D printed materials can transform their structure in response to specific stimuli, such as pressure, temperature, pH, or light radiation. The wide panorama also includes functional 3D materials, able to create printable scaffolds that have intrinsic functionality, e.g., with biorecognition capabilities. The combination of 3D printing technology with accurate materials engineering allows for obtaining constructs that closely mimic the dynamics of native tissues.[31] Since the fundamental importance of stiffness in tissues and pathology development, in this review, we show how mechanical properties of 3D matrices could be modulated to mimic tissue-specific features.

2. TISSUE STIFFNESS MEASUREMENT

Numerous diseases are associated with changes in tissue stiffness. This aspect has been usually assessed in clinical practice by palpation or visual examination, which are subjective and nonquantifiable methods. In recent years, objective and noninvasive methods have been introduced to quantify tissue mechanical properties *in vivo* and map them, based on the use of elastography.[32,33] As described in their review by Sigrist and colleagues, elastography assesses the capability of a tissue to resist deformation (tissue elasticity). According to the types of deformation applied, three kinds of elastic modulus are derived: (1) Young modulus ($E = \sigma_n/\varepsilon_n$) defined as materials' stiffness as given by the ratio of normal stress to normal strain; (2) shear modulus ($G = \sigma_s/\varepsilon_s$) defined as materials' resistance to deformation as given by the ratio of tangential force to shear strain and (3) bulk modulus ($H = \sigma_v/\varepsilon_v$) defined as materials' resistance to compression as given by the ratio of volumetric stress to a volumetric strain. Considerable for soft tissues is the Poisson's ratio ($\nu = -\varepsilon_{trans}/\varepsilon_{axial}$) defined as the ratio of transverse strain to axial. It describes the tendency of a solid to retain its original volume. Usually, Poisson's ratio for soft tissues is around 0.5 because of their high water content, and its value allows to estimate Young's modulus from shear modulus, as $E = 3G$.[34] Schematic representation of the directional elastic properties of materials: Young modulus E, Shear modulus G, Bulk modulus H and Poisson's ratio ν, are summarized in Figure 2. Elastography is

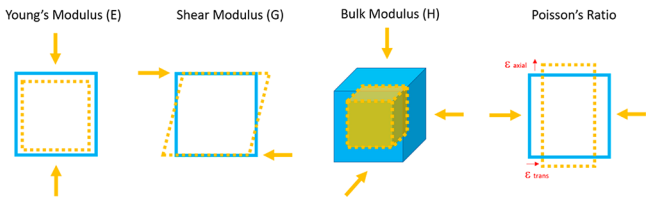

Figure 2. Schematic representation of the directional elastic properties of materials: Young modulus E, Shear modulus G, Bulk modulus H and Poisson's ratio ν. The arrows represent the direction of stress exerted.

defined by the excitation types and the measured physical quantity. For example, strain elastography measured deformation after manual compression, cardiovascular pulsation, or respiration. Instead, shear wave imaging estimated the rate of propagation of shear wave into the tissue.[35]

2.1. Quasi-static Elastography. Over the years, several techniques have been developed to measure tissue's mechanical properties, and one of them is quasi-static elastography. It relies on the acquisition of radiofrequency before and after the application of a small amount of quasi-static deformation. Tissue composition, water content, time required for the measurement, and parameter settings may influence the results; thus, an increasing number of studies proposed new

https://dx.doi.org/10.1021/acsabm.0c01472
ACS Appl. Bio Mater. 2021, 4, 2233−2250

approaches to improve the technique and standardize the results.[36−38]

2.2. Magnetic Resonance Elastography. Magnetic resonance elastography (MRE) is another noninvasive method to detect tissue stiffness and consists in the generation of shear waves of specific frequencies and in the acquisition of wavefield inside the tissues. Because of the nature of deformation, the outcome is the shear modulus (G) of the tissue.[39,40] Specifically, after the induction of shear waves into the tissue using an external device, waves inside the body are imaged and processed to obtain quantitative images. Algorithms based on an equation of motion allowed to calculate mechanical properties considering the tissue homogeneous, isotropic, and incompressible. MRE potentialities are linked to its flexibility and noninvasiveness.[41]

2.3. Other Elastography Techniques. Transient elastography (TE) is based on vibration at low frequencies and links wave velocity to tissue stiffness,[42] while shear wave elastography (SWE) gives information about E and G through shear wave velocity.[43] TE is a painless, easy-to-use, and rapid technique. A transducer probe transmitted the vibration to the tissue inducing wave propagation, and stiffness is correlated to the propagation speed. Stiffer tissues have faster shear wave propagation. However, in obese patients, the measurement is more difficult, leading to a higher error percentage.[44] Shear Wave Elastography (SWE) gives information about E and G through shear wave velocity.[43] SWE measures the displacement of tissues caused by external pressure or the radiation force from a focused ultrasound beam, leading to highly localized displacement. Then, the wave's propagation is detected by an ultrasound transducer. This approach has been used for the analysis of prostate, liver, and cardiac tissue.[45] Furthermore, Harmonic Motion Imaging (HMI) method is based on an oscillatory radiation force that induces harmonic tissue motion. The advantages are the possibility to reach deeper organs, such as the pancreas, and to avoid respiratory artifacts that generally produce static motion. Moreover, displacement amplitude is directly linked to tissue stiffness.[46,47]

Several studies tried to compare various techniques to identify the more suitable diagnosis of disease progression when stiffness changes occur. For instance, it has been reported that MRE is more efficient than TE in liver fibrosis detection,[48−50] and O'Hara et al. stated that TE and SWE are comparable in the detection of hepatic fibrosis and cirrhosis.[51]

3. TISSUE MECHANICAL PROPERTIES

As already discussed, the tissues and the cells they are made of are continuously subjected to physical forces such as compression and tension. Cells respond to these stimuli, dynamically adapting to them and modifying their microenvironment. It has been shown that mechanical properties of tissues are profoundly correlated with their development, homeostasis, risk of disease, and response to therapeutic treatments.[52] Since matrix elasticity influenced cell function, stem cell differentiation, and activation of several intracellular pathways, mechanosensing plays an important role in cell functionality.[53] Modification in microenvironment rigidity resulted in changes in the conformation of adhesion components (e.g., vinculin, integrins, and focal adhesion kinase or FAK) that activated proteins involved in mechanotransduction. For instance, on a stiff matrix, two traducers called YAP and TAZ translocated into the nucleus to induce the transcription of genes involved in many cellular processes including proliferation, metabolism regulation, and differentiation.[54] Further, in response to mechanical stimuli, Rho/ROCK pathway promoted cytoskeleton activation regulating, for example, the differentiation of stem cells.[55] Rigid substrates promoted the differentiation of white adipocyte into beige type regulating cell spreading and thermogenic genes expression.[56] Additionally, adipogenesis and osteogenesis of mesenchymal stem cells (MSCs) in 3D culture were controlled by matrix stiffness through the modulation of integrin, FAK, actin myosin contractility, nuclear laminin, and intracellular pathway such as YAP-TAZ.[57] Further, the commitment of MSCs toward sweat gland cells was promoted by a stiffer matrix by YAP-dependent mechanotransduction.[58]

Specific cell types were subjected to complex mechanical cues because of the localization and the matrix composition. For instance, endothelial cells responded to these stimuli with the activation of ion channels, G-proteins and G-protein coupled receptors, integrins, and intracellular junction proteins.[59] Stiffness also influences autophagy, a catabolic mechanism that regulates cellular homeostasis, motility, and differentiation. Stiff substrates decreased autophagy in vascular endothelial cells; meanwhile, softer ones promoted it and the endothelial phenotype, suggesting that increasing rigidity affects endothelial function. Contrariwise, stiffer substrate promoted autophagy in vascular smooth muscle cells underlining the importance of rigidity in the control of specific cell behavior.[60]

ECM rigidity plays an important role also during pathology development. For instance, pulmonary fibrosis, characterized by fibroblast activation, is associated with excessive collagen deposition. Hence, changes in matrix composition resulted in an increased rigidity. In this context, several intracellular pathways associated with mechanotransduction were activated, including Rho/ROCK, YAP-TAZ, and MRTF-A.[61] In the following paragraphs, the tissues that best show this behavior and that have been studied more thoroughly will be described in detail, except for the liver, which has been the subject of extensive reviews and systematic analysis.[62,63]

3.1. Breast. The ECM of mammary tissue is composed of several proteins that are responsible for its structure and function as well described in the review by Insa-Rodrìguez and Oskarsson.[64] Particularly, this tissue is sustained by collagens, fibronectin, laminins, glycosaminoglycans and proteoglycans, matricellular proteins, and ECM remodeling enzymes. It is widely accepted that during tumor progression, changes in ECM composition cause stromal stiffening; the normal mammary gland has an elastic modulus between 160 and 200 Pa,[65] but its stiffening is associated with a higher risk of tumor development.[66] Furthermore, human epidermal growth factor receptor 2 (HER2)-positive tumors and triple negative breast cancer (TNBC), the two more aggressive tumor subtypes, show higher stiffness (>5 kPa), mainly caused by collagen deposition, linearization, and bundling.[19] Chen and colleagues analyzed the stiffness of breast cancer subtypes using SWE. TNBC showed a higher average mean stiffness (165.8 ± 48.5 kPa) when compared to Estrogen Receptor (ER)-positive (136.9 ± 57.2 kPa) and HER2+ tumors (160.3 ± 56.2 kPa). Moreover, it has been seen that stiffness is correlated to tumor size, histological grade, and lymph node involvement.[20] Finally, several *in vitro* studies have reported matrix stiffness as a critical aspect in the regulation of spheroids

https://dx.doi.org/10.1021/acsabm.0c01472
ACS Appl. Bio Mater. 2021, 4, 2233−2250

formation,[67−70] integrin signaling, cell morphology,[65] stromal and cancer cell interactions,[71] and drug resistance.[72]

3.2. Brain. As described by Rape et al., brain ECM is mainly composed of hyaluronic acid (HA) and in minor degrees by laminin, fibronectin, and collagen IV and V.[73] Brain mechanical measurements are quite difficult because of tissue heterogeneity and physiological position. For instance, McIlvain and colleagues measured stiffness starting from images acquired by MRE. They observed shear stiffness values that ranged from 2.48 to 4.11 kPa, with the cerebrum and cerebral lobes exhibiting a higher stiffness compared to the cerebellum.[21] Chauvet and colleagues measured the Young's Modulus of four brain tumor types, meningiomas, low-grade gliomas, high-grade gliomas, and metastasis by SWE; the obtained values were 33.1 ± 5.9 kPa, 23.7 ± 4.9 kPa, 11.4 ± 3.6 kPa, and 16.7 ± 2.5 kPa, respectively, which were higher than the one found in normal brain (7.3 ± 2.1 kPa).[74] Moreover, Tabet et al. analyzed the brain's and tumor's storage moduli, which were 189 and 536 Pa, respectively.[75] GBM tumoral progression was demonstrated to be strongly correlated to mechanosensing and matrix stiffening;[76−78] in fact, changes in scaffold stiffness caused the modulation of glioblastoma cell morphology, proliferation and spheroid formation, gene expression and drug resistance.[79,80]

3.3. Lungs. Lung ECM is mainly composed of collagen (type I, II, III, V, and XI) and glycoproteins such as fibrillin. Specifically, the alveolar interstitial part mostly consists of collagen types I and III, fibronectin, and elastin. Instead, cancerous tissue shows a higher level of collagen, hyaluronan, tenascin C and fibronectin;[81] at the same time, dense stroma and fibrosis are common in lung adenocarcinoma. Angel and colleagues showed that the first alteration occurring in the early stage of lung adenocarcinoma is the deposition of collagen-containing hydroxylated prolines, which are involved in fibrosis. Besides, they confirmed the presence of a higher amount of collagen type I in tumor tissue.[82] Lung stiffness could be measured using MRE, assessing a shear stiffness at rest volume of 0.93 ± 0.22 kPa, whereas at total lung capacity was 1.41 ± 0.41 kPa.[83] Moreover, atomic force microscopy (AFM) indentation tests quantified the elastic modulus of healthy lungs around 1 kPa, while fibrosis could increase the stiffness to values of 13−17 kPa.[84,85] The substrate stiffness influences cell behavior, such as growth,[86] migration,[87,88] and epithelial-to-mesenchymal transition.[84]

3.4. Pancreas. Pancreatic ECM is mainly composed of collagen types I, III, IV, and V and different types of laminin,[89] and during cancer progression, various alterations in the composition of ECM occur. For instance, adenocarcinoma-associated fibroblasts produced ECMs oriented in a parallel pattern, with fibrillar collagen types I and III, which were progressively increased during tumoral progression, and differences were also detected in glycoprotein and proteoglycan components.[90,91] Adenocarcinoma showed higher stiffness (3.78 kPa) compared to normal pancreatic tissue (1.24 kPa), and its mechanical properties were also influenced by unhealthy habits such as smoking and alcohol consumption and by metabolic alterations due to diabetes.[92−94] Itoh and colleagues employed the MRE technique to estimate the mechanical properties of normal and tumoral tissue; the authors showed that a healthy pancreas had an overall stiffness of 2.47 ± 0.11 kPa, whereas a tumoral one had a stiffness of 6.06 ± 0.49 kPa.[95] Furthermore, matrix stiffness could induce epithelial-to-mesenchymal transition, invasion capability, and chemoresistance.[94,96]

4. 3D MATRIX STIFFNESS MEASUREMENTS

To better resemble mechanosensing that occurs *in vivo*, an ideal 3D matrix mimics the mechanical properties of the original tissue or of the pathological environment that is studied. Several techniques have been adapted to measure the elastic modulus of *in vitro* scaffolds to understand whether their stiffness is comparable to the one of interest. Particularly, hydrogels are the most widely used matrices for 3D culture because of their biocompatibility, composition, porosity, water content, and tunable properties.[97,98] In the next section, we summarize the most used methods to measure the mechanical properties of hydrogels.

4.1. Tensile and Compression Test. The tensile test is a widely used method for the evaluation of Young's modulus, which is measured as the ratio of applied stress to resultant strain (N/m^2). Soft biological tissues usually display increased resistance to deformation as the applied stress increases. During tensile tests performed on biological samples, a strain is best measured at given stress considering the material as perfectly elastic, and for this reason, stress and strain applied must always be indicated.[99] For instance, Czichy and colleagues prepared cylindrical samples with definite diameter and length, i.e., 4.7 mm and 18 mm, respectively. The authors performed tensile tests using an AntonPaar MCR 301 to calculate the Young's modulus of alginate−methylcellulose scaffolds with embedded magnetic microparticles, considering the linear part at the beginning of the stress−strain curve.[100] Fu and colleagues conducted tensile measurement using an Instron-5500R tensometer. Specifically, they obtained ring shape samples of their protein-based hydrogel (d_{in} = 8 mm, d_{out} = 10 mm, h = 3 mm), and after overnight storage in PBS, they calculated Young's modulus at 15% strain with an extension rate of 25 mm/min.[101] Instead, Chen et al. used a universal mechanical testing machine with a 10 kg load cell. Young's modulus was assessed at 5% of strain, keeping the rate of stretch constant at 50 mm/min.[102]

The compression test is another method commonly used to measure hydrogel elastic modulus. As well as for tensile tests, samples should be prepared with definite shape and dimension. For example, Nguyen et al. prepared their PEG-based hydrogels into PTFE cylindrical molds with 11.50 mm in height and 11.00 mm in diameter. The samples were then compressed with a strain rate of 2.0 mm/min using an Instron 3344, and the elastic moduli (E) were calculated within 10% strain.[103] Tirella and colleagues analyzed cylindrical hydrogels made of PEG (5 mm in diameter and 3 mm in height) with uniaxial unconfined compression. Force and displacement were recorded normalized to the cross-sectional area and initial length of the samples. The compression modulus was measured in the region where stress varied linearly with the applied strain.[104]

4.2. Atomic Force Microscopy. Atomic force microscopy (AFM) is a widely used technique based on a thin cantilever with a tip that interacts with the sample; the resultant force is measured and then used to derive mechanical properties. Importantly, probe features (e.g., material, spring constant, radius, and cone angle) influence resolution, accuracy, and sensitivity of the measurement.[105] Suriano and colleagues used a commercially available probe with a colloidal SiO_2 tip, with a radius of 2.71 μm and a spring constant of 0.0412 N/m

https://dx.doi.org/10.1021/acsabm.0c01472
ACS Appl. Bio Mater. 2021, 4, 2233−2250

Table 1. List of the Approaches Used to Modulate Mechanical Properties of Alginate Hydrogels

materials	concentration	preparation method	range of elastic modulus	measure technique	cells	ref
alginate (Alg)	0.5, 1, and 2 wt %	$CaCO_3$ with D- glucono-δ-lactone cross-linking	1.85−5.29 kPa	Frequency sweep (0.1−100 Hz at 0.5% strain)	breast cancer cells	68
Alg	Alg: 0.75 wt %	$CaCO_3$ with D- glucono-δ-lactone cross-linking	5.8 kPa	frequency sweep (0.1−100 Hz at 0.5% strain)	breast cancer cells	68
collagen (Col)	Col: 1 mg/mL					
Alg	Alg: 0.8, 1.3, 1.8, and 2.3 wt %	$CaCL_2$ cross-linking	1.4−14,2 kPa	compression test (speed 1 mm/min)	hMSCs	120
gelatin (Gel)	Gel: 4.1 wt %					
Alg	Alg: 1, 3, 5, 7, and 9 wt %	$CaCL_2$ cross-linking	29.8−48 kPa	compression test (speed 0.1 mm/s)	MSCs	121
Gel	Gel: 2, 4, 6, 8, and 10 wt %					
Alg	Alg: 1, 3, and 5 wt %	$CaCl_2$ cross-linking	5.86−22.88 kPa	indentation (probe 500 μm)	breast cancer cells	69
Gel	Gel: 5, 7, and 9 wt %					
Alg	Alg: 4%	gelation	0.2−2 kPa	frequency sweep (0.05−500 rad/s at 5% initial straing)	MDA-MB-231 (breast cancer cells)	72
Matrigel $CaCl_2$- containing liposome	Matrigel: 25%	$CaCl_2$ cross-linking				
Alg	Alg: 5 mg/mL	$CaCl_2$ cross-linking	1.2−9.8 kPa	compression test	MDA-MB-231 (breast cancer cells)	122
Col	Col: 3 mg/mL					
norbomene- modified Alg with an enzymatically degradable peptide	different combinations of degradable peptide, cross-linker, and low and high molecular weight alginate	UV cross-linking	0.57−13.90 kPa	compression test (speed 0.016 mm/s until 10% strain)	fibroblast	124
Alg and chondroitin sulfate (CS)	AL: 3 wt %	physical cross-linking	50−120 kPa	AFM	chondrocytes	125
	CS: 5 wt %					
aldehyde-modified Alg	20 mg/mL	hydrazone cross-linking	0.9 kPa	compression test (speed 10 mm/min until 70% stram)	human neuronal cells	126

https://dx.doi.org/10.1021/acsabm.0c01472
ACS Appl. Bio Mater. 2021, 4, 2233−2250

Table 2. Table Summarizing the Main Strategies to Modulate SF Hydrogel Stiffness

materials	concentration	preparation method	range of elastic modulus	measure technique	cells	ref
silk fibroin (SF)	1.5−4 wt %	high-pressure CO_2	6−64 kPa	compression test (speed 20 μm/s until 60% strain)	MSCs	131
SF and tyromine-conjugated SF	from 0 to 50 mg/mL (various ratio)	HRP-cross-linking	0.3−21.8 kPa	compression test	BMSCs	132
SF collagen (Col)	various ratio starting from SF 70 mg/mL collagen 7.8 rug/mL	gelation	9.93−31.16 kPa	AFM (tips 5 urn, force constant 0.03 N/m)	BMSCs	133
SF Col	5−10 mg/mL 1 mg/mL	sonication and gelation	0.2−0.7 kPa	compression test	breast cancer cells	134
SF Col	SF 0.175−2.45 wt % collagen 0.5−3.5 mg/mL	sonication and gelation	0.05−20.4 kPa	compression test (0.1 mm/min)	hMSCs	135
SF SF nanofiber (SFN)	2 wt %	freeze-drying	3−58.4 kPa	compression test (speed 5 mm/min)	BMSCs differentiation in endothelial cells	136
SFN	5 wt %	concentrating SFN solution and salt-leaching	2−18 kPa	compression test (speed 2 mm/min until 30% strain)	BMSCs myogenic differentiation	137
SF SFN	various ratio starting from 6% (SF) and 2% (SFN)	HRP-cross-linking	9−60 kPa	frequency sweep (0.1−100 rad/s)	BMSCs differentiation in different lineages	138
SFN	1, 2, and 4 wt %	HRP-cross-linking	0.6−160 kPa	frequency sweep (0.1−100 rad/s)	BMSCs	139

measured with the Sader method. According to the nature of the sample, they derived Young's modulus using Derjaguin−Müller−Toporov and the Johnson−Kendall−Roberts models for low or high surface energy, respectively.[106] Thanks to its level of resolution, AFM has been used to assess the elastic modulus of hydrogels. For instance, Galuzzi et al. measured the local elasticity of poly(*N*-isopropylacrylamide) (PNIPAM) hydrogels using a commercial AFM Dimension Icon. A force curve was obtained at every point of a matrix in a selected area of the sample to reconstruct the mechanical properties according to the morphology. Probes with different geometries were then used to fit the indentation curve and derive Young's modulus; the Hertz model was used for spherical probes and the Sneddon model for sharp ones, assuming a Poisson's ratio of 0.5 and a linear relationship between stress and strain.[107] As also described by Market et al., the Hertz model was used to derive elastic properties of their hydrogels consisting of different biomaterials; the model takes into consideration the sphere radius (R), the force (F), the elastic modulus of the sample surface (E), the Poisson's ratio (ν) which is assumed to be 0.5 for hydrogel and the indentation (δ).

$$F = \frac{4E\sqrt{R}}{3(1-\nu^2)}\delta^{3/2}$$

After AFM measurement, cantilever deflection (d) and piezo movement (z) were obtained. So, with Hooke's law, $F = k \times d$, applied force (F) is calculated from the deflection. Moreover, indentation (δ) was derived from $z = d + \delta$. So, the elastic modulus was derived using the following equation:[108]

$$F = \frac{4E\sqrt{R}}{3(1-\nu^2)}\left(z - \frac{F}{k}\right)^{3/2}$$

4.3. Nanoindentation. Like AFM, the nanoindentation technique is particularly useful for analyzing the microenvironment and how its localized influence affects the mechanical behavior of the matrix.

Nanoindentation can be used for mapping the elastic properties of soft materials at a microscopic scale. This technique allows the precise application of a defined force by an indenter tip, while simultaneously measuring the indentation depth into the sample substrate with subnanometer accuracy. In order to measure soft samples having low Young's modulus, flat punches and spherical indenters with a relatively large radius have been developed.[109] Nanoindentation shows some limits such as the evaluation of the viscoelastic models, the choice of the right calibration material, and events of adhesion between the sample and the probe (especially if soft and hydrated). Kaufman and colleagues tried to overcome these limitations by looking for the best model to link macroscopic and microscopic properties and by assessing the capability of these techniques to discriminate materials with similar mechanical properties, showing promising results.[110] Specifically, the work showed that, although nanoindentation is a widely used technique for the mechanical characterization of biomaterials, in the case of hydrated samples, the measurements are not yet so reliable. With some tricks, such as the use of the right reference materials, Kaufman showed how nanoindentation can also be used to discriminate hydrogels with a low modulus similar to each other in hydration conditions.[110−112] Karavasili and colleagues analyzed the elastic modulus of hydrogels using a Shimadzu DUH211S device with Berkovich diamond indenter whose tip radius was 100 nm, obtaining a resolution of 0.196 μN. The tests involved loading under force-controlled, and the outcomes are force-depth curves, particularly, indentation depth varied from 7 to 25 μm with a loading rate of 0.35 mN/s, until 1 mN. The object of the study was to use a numerical-experimental approach to obtain a complete physical-mechanical characterization of 3D printable alginate−methylcellulose hydrogels with bioactive components. In detail, nanoindentation tests have been made more accurate thanks to the support from finite element analysis simulation.[113]

4.4. Rheology. To analyze the mechanical properties of bulk 3D matrix, it is not possible to follow an approach such as AFM and nanoindentation, as the latter provides nanometer resolution. To accurately analyze the mechanical properties of 3D samples in bulk, the most suitable technique is the shear

https://dx.doi.org/10.1021/acsabm.0c01472
ACS Appl. Bio Mater. 2021, 4, 2233−2250

Table 3. Table Summarizing the Main Strategies to Modulate GelMA Hydrogel Stiffness

materials	concentration	preparation method	range of elastic modulus	measure technique	cells	ref
GelMA	5, 10, and 15 wt %	photo-cross-linking	1.7−16.4 kPa	compression test (speed 0.01 nun/s until 10% strain)	dental stem cells	142
GelMA	7.5, 10, and 15 wt %	photo-cross-linking	25.59−41.78 kPa	uniaxial compression test (speed 1 mm/min until 50% strain)	BMSCs differentiation into endothelial cells	144
GelMA	5, 10, 20, and 30 wt %	photo-cross-linking	3.08−184.52 kPa	uniaxial compression test (speed 1 mm/min)	PC12 (adrenal gland)	145
GelMA	10 wt %	photo-cross-linking	3.5−13.1 kPa 5.4−18.5 kPa	AFM (tips 200 um, resonant frequency 17 kHz, force constant 0.08 N/m)	human adipose- derived stem cells	146
GelMA PEGDA	GelMA 0.05−0.5 wt % PEGDA 5−15 wt %	photo-cross-linking	1.6−25 kPa	compression test (speed 2 mm/min until 2.5% strain)	osteoblast and osteosarcoma cells	147,148
GelMA PEGDA	GelMA 1−5 wt % PEGDA 1−15 wt % (several combination)	photo-cross-linking	0.1−8 kPa	frequency sweep (1−400 rad/s)	MDA-MB-231 (breast cancer cells)	149
GelMA silk fiber (SF)	GelMA 6 wt % SF of different length 20 mg	photo-cross-linking	7.08−19.34 kPa	compression test (speed 0.1 mm/min until 10% strain)	osteoblasts	150

rheology.[114] Rheology is the study of how a material deforms when forces are applied to it. Thus, applying shear stress to a 3D matrix can be helpful in the determination of elastic modulus (stiffness) as well as viscous properties of a bulk 3D tumor tissue.

However, it must be considered that the soft tissues behave as nonlinear, anisotropic, and nonuniform viscoelastic materials.[115] Consequently, their mechanical properties depend on deformation and deformation rate. In the case of soft materials, this implies problems in the reproducibility and reliability of measurements and interpretation of results. Therefore, rheology may not be considered as a standard measurement technique for evaluating the mechanical properties of soft matrices. In recent years, research groups are focusing their attention on the development of new algorithms and solutions to take into consideration the inhomogeneous and anisotropic nature of rheology in this field. As well explained in the work of L. Bilston, the rheological behavior of soft tissues is very complex and strongly influences the analysis and interpretation of elastography measurements. To overcome this bias and, thus, to obtain reliable and repeatable experimental measurements, there are some key elements that must be taken into consideration: first, the influence of tissue load and strain on measurements and then other parameters such as intrinsic tissue characteristics, such as inhomogeneity and anisotropy. The current frontier in this area is related to the development of new algorithms to be able to consider the complexity, inhomogeneity, and anisotropy of soft materials. Unfortunately, research is still a long way from refining elastography further so that it can be used as a tool for understanding microstructural changes in tissues.[116]

5. 3D MATRIX WITH TUNABLE STIFFNESS

According to tissue properties, such as matrix composition and stiffness, cells require specific culture conditions and materials that better resemble features of the tissue of origin. Moreover, hydrogels and scaffold properties (e.g., swelling ratio, pore size, stiffness) must be fully characterized to strictly regulate cell culture conditions. Here, we focused on stiffness and its role in cellular behavior, showcasing different materials and approaches to obtain constructs with tunable stiffness. At the end of each paragraph, tables summarized the main strategies used to obtained hydrogels with different mechanical properties (i.e., Tables 1, 2, 3, 4, and 5 for alginate, silk, GelMA, hyaluronic acid, and peptide-based as well as PEG-based hydrogels, respectively).

5.1. Alginate. Alginate is a linear anionic polysaccharide copolymer deriving from brown seaweeds and made of β-(1−4)-D-mannuronic acid (M-blocks) and α-L-guluronic acid (G-blocks); the ratio and the sequence of blocks influence the properties of the alginate. Hydrogels could be obtained with different methods, among which ionic or covalent cross-linking, phase transition, cell cross-linking, free-radical polymerization, and click-chemistry.[117] Alginate hydrogels have good printability and biocompatibility, and they are used, for example, in vascular, cartilage, and bone tissue printing. Some drawbacks of these scaffolds are low cellular adhesion, slow degradation rate, and poor mechanical properties, especially for mimicking bone features. To overcome these limitations, alginate could be chemically modified or cross-linked by means of different strategies.[118] Alginate is widely used for its fast cross-linking; however, the lack of cell-adherent motifs limited its use for cell and tissue culture.[119] To overcome this limitation, some authors used alginate hydrogel containing arginylglycylaspartic acid (RGD) peptide, which mediates cell adhesion,[51] or gelatin, which presents the same sequence.[69,120,121]

Various approaches may be adopted to obtain hydrogels with tunable mechanical properties. As an example, Khavary and colleagues studied the effect of different stiffnesses and hydrogel compositions on multicellular aggregate formation; the stiffness was proportional to alginate concentration, and stiffer hydrogels supported the growth of larger aggregates. Moreover, the authors observed that adding RGD peptide increased cellular adhesion and accelerated cell proliferation but not the dimension of formed spheroids which depended only on stiffness.[68] Interestingly, a composite hydrogel that consisted of different alginate concentrations and fixed gelatin amounts showed a wide range of compressive moduli (from 1.4 to 14.2 kPa), but higher viability of human mesenchymal stem cells (HMSCs) was found in the scaffold with lower stiffness.[120] Di Giuseppe et al. showed that the compressive modulus of alginate−gelatin composite hydrogel depended both on cross-linking time and precursors concentration.[121] Finally, Jiang and colleagues analyzed how alginate influenced elasticity and the formation of tumor spheroids. Particularly, they tuned the elastic modulus from 5.46 to 22.88 kPa increasing alginate concentration from 1 to 5 w%. Moreover,

https://dx.doi.org/10.1021/acsabm.0c01472
ACS Appl. Bio Mater. 2021, 4, 2233−2250

Table 4. Table Summarizing the Main Strategies to Modulate HA Hydrogel Stiffness

materials	concentration	preparation method	range of elastic modulus	measure technique	cells	ref
alginate (Alg)	0.5, 1, and 2 wt %	$CaCO_3$ with D-glucono-δ-lactone cross-linking	1.85−5.29 kPa	frequency sweep (0.1−100 Hz at 0.5% strain)	breast cancer cells	68
Alg collagen (Col)	Alg: 0.75 wt % Col: 1 mg/mL	$CaCO_3$ with D-glucono-δ-lactone cross-linking	5.8 kPa	frequency sweep (0.1−100 Hz at 0.5% strain)	breast cancer cells	68
Alg gelatin (Gel)	Alg: 0.8, 1.3, 1.8, and 2.3 wt % Gel: 4.1 wt %	$CaCl_2$ cross-linking	1.4−14.2 kPa	compression test (speed 1 mm/min)	hMSCs	120
Alg Gel	Alg 1, 3, 5, 7, and 9 wt % Gel 2, 4, 6, 8, and 10 wt %	$CaCl_2$ cross-linking	29.8−48 kPa	compression test (speed 0.1 mm/s)	MSCs	121
Alg Gel	Alg: 1, 3, and 5 wt % Gel: 5, 7, and 9 wt %	$CaCl_2$ cross-linking	5.86−22.88 kPa	indentation (probe 500 μm)	breast cancer cells	69
Alg Matrigel $CaCl_2$- containing liposome	Alg: 4% Matrigel: 25%	gelation $CaCl_2$ cross-linking	0.2−2 kPa	frequency sweep (0.05−500 rad/s at 5% initial straining)	MDA-MB-231 (breast cancer cells)	72
Alg Col	Alg: 5 mg/mL Col: 3 mg/mL	$CaCl_2$ cross-linking	1.2−9.8 kPa	compression test	MDA-MB-231 (breast cancer cells)	122
norbornene-modified Alg with an enzymatically degradable peptide	different combination of degradable peptide, cross-linker and low and high molecular weight alginate	UV cross-linking	0.57−13.90 kPa	compression test (speed 0.016 mm/s until 10% strain)	fibroblast	124
Alg and chondroitin sulfate (CS)	AL: 3 wt % CS: 5 wt %	physical cross-linking	50−120 kPa	AFM	chondrocytes	125
aldehyde-modified Alg	20 mg/mL	hydrazone cross-linking	0.9 kPa	compression test (speed 10 mm/min until 70% strain)	human neuronal cells	126

https://dx.doi.org/10.1021/acsabm.0c01472
ACS Appl. Bio Mater. 2021, 4, 2233−2250

Table 5. Table Summarizing the Main Strategies to Modulate Peptide-Based, PEG-Based, and Dextran-Based Hydrogel Stiffness

materials	concentration	preparation method	range of elastic modulus	measure technique	cells	ref
L-histidine tripeptide Succinic acid	peptide: 8.6 μmol acid: 4.3 μmol	gelation	0.87−9.7 kPa	frequency sweep (8−100 rad/s)	NIH 3T3 (fibroblasts)	161
Fmoc-tyrosine-lysine Fmoc-tyrosine-aspartic	5, 10, and 15 mM	self-assembling	4−62 kPa	amplitude sweep	hepatoma cell lines	162
self-assembly peptide (EFK8)	1.25, 5, and 10 mg/mL	self-assembling	0.04−0.1 kPa	microindentation	NIH 3T3 (fibroblasts)	163
collagen-like peptide polymer	1 wt %	overnight annealing	40.6−709 kPa	frequency (0−10 Hz) and strain (0.1−100%) sweep	MDA-MB-231 (breast cancer cells)	164
peptide amphiphiles conjugated with host−guest motifs	1 wt %	self-assembling	2.8−5.1 kPa	frequency (0−100 Hz) and strain (0.01−10%) sweep	NIH 3T3 (fibroblasts)	166
PEG-norbornene PEG thiol	different ratio and photoinitiator concentration	thiol−ene reaction	1.5−12.6 kPa	frequency and strain sweep	cardiomyocytes	168
PEG modified with host−guest motifs	various composition	thiol-allylether photo-cross-linking	2.3−6.5 kPa	frequency sweep	MIN6 (pancreatic B-cells)	169
GelMA methacrylic dextran (DeMA)	GelMA: 6−10 wt % DeMA: 1 wt %	photo-cross-linking	0.6−42.3 kPa	compression test (speed 1 mm/min)	induced hepatic progenitor cells	173
dextran vinyl sulfone	0.7 g/mL	photo-cross-linking	0.77−11.03	microindentation	NHLFs (myofibroblast)	174

the adding of different percentages of gelatin changed the number of cellular adhesion sites without having an impact on the mechanical properties of the hydrogel. Meanwhile, hydrogels with an elastic modulus of 7.92 kPa and the highest gelatin concentration (alginate 1 wt %, gelatin 5 wt %) allowed the formation of the largest and the most viable tumor spheroids.[69]

Hydrogels with dynamic mechanical properties were used to study the insurgence of drug resistance in breast cancer cells. For instance, Joyce and colleagues developed a dynamic alginate−Matrigel system in which stiffening was induced by the cross-linking of calcium-loaded liposomes present into the hydrogel due to exposure to near-infrared light. A breast cancer cell line, named MDA-MB-231, was grown in a dynamically stiffened hydrogel and showed a decreased sensitivity to a chemotherapeutic drug, called doxorubicin, when the elastic modulus was increased to mimic the early stage of breast tumor. In addition, cell cultures in this condition also expressed markers of mesenchymal phenotype.[72]

The degree of cross-linking strongly influences the degradable features and the mechanical properties of alginate hydrogels. Liu et al. succeeded in tuning the mechanical properties of alginate−collagen composite hydrogel by changing the amount of cross-linker; actually, the authors were able to enhance the Young's modulus of the gel from 1.2 to 9.8 kPa by increasing the $CaCl_2$ concentration.[122] Fletcher et al. also demonstrated that variations of gelling time could influence material's mechanical properties. The storage modulus of hydrogels derived from a polyelectrolyte complex, composed of alginate and chitosan, was 6.5-fold increased when cross-linked at high temperature (complexes prepared at 50 °C compared to 37 °C).[123] Lueckgem and colleagues combined norbornene-modified alginate and peptide sequences with thiol-containing cysteines at either end to induce UV cross-linking via thiol−ene chemistry. Additionally, the peptide sequences were enzymatically degradable to allow hydrogel modification by the cells. This combination led to the realization of gels with an elastic modulus that ranged from 0.57 to 13.90 kPa.[124] To achieve higher stiffness, Ma and colleagues used strontium alginate/chondroitin sulfate to produce hydrogels through physical cross-linking, and the concentration of both strontium chloride and the presence of chondroitin sulfate (CS) strongly influenced the elastic modulus. Indeed, the addition of CS allowed to reach the value of 120 kPa and caused a decrease in pore size compared to strontium alginate hydrogels. Also, CS and strontium increased the proliferation and reduced the apoptosis of chondrocytes, resulting in a good candidate for cartilage transplants *in vivo*.[125]

Dissimilarly, other cell lines require softer culture conditions to grow or proliferate. As an example, aldehyde-modified alginate hydrogels could be used to obtain scaffolds with an elastic modulus of 0.9 kPa through hydrazine cross-linking. The biocompatibility of hydrazine, the fast cross-linking, and the brain-like stiffness exhibited by the material supported human neuronal cells viability and neurite outgrowth.[126]

5.2. Silk. The advantages of silk fibroin (SF) hydrogels as a biomaterial are well depicted in the review of Kapoor and Kundu. SF represents a good candidate for the fabrication of hydrogels with good elasticity and strength due to the presence of crystalline regions associated with less organized.[127,128] This organization was derived from hydrogen and hydrophobic interactions between protein chains. Moreover, hydrogel properties could be modulated by changing the source of the silk (e.g., cocoons or silk glands of different silkworm species), its concentration, and preparation method (e.g., pH, temperature, and ionic strength variation). As a result, silk-based hydrogels show tunable mechanical properties, slow degradation rate, and high permeability to oxygen and other molecules, which make them suitable from 3D cultures.[129] Since several preparation methods have been developed to modified SF hydrogel mechanical properties, in their review, Johary and colleagues well characterized the advantages and disadvantages of different approaches. For example, physical cross-linking is safe, inexpensive, and less toxic for cells. However, it needs time, and the kinetic of the reaction could not be controlled.

https://dx.doi.org/10.1021/acsabm.0c01472
ACS Appl. Bio Mater. 2021, 4, 2233−2250

Instead, enzymatic cross-linking (e.g., HRP) provides high elasticity and tunable stiffness. The reaction may be modulated by modifying ionic strength, pH, or the temperature. Finally, chemical cross-linking (e.g., genipin and glutaraldehyde) allows the formation of stronger bonds, and stiffer hydrogel although higher cell toxicity may be observed.[130] It is reasonable to consider SF a good candidate for the fabrication of hydrogels with tunable stiffness. In particular, the modulation of silk concentration and/or the variation of the preparation protocol allows reaching the desired mechanical properties. Floren and colleagues obtained SF hydrogels with tunable stiffness (6−64 kPa) by changing the starting silk protein concentration. The hydrogels retained structural parameters (e.g., matrix pore size and β-sheet crystallinity) among different SF concentrations, but only the mild-range stiffness (33 kPa, SF 3%) was able to strongly increase human mesenchymal stem cell commitment to smooth muscle cell phenotype.[131] Hasturk et al. observed that increasing the ionic strength of buffer solution used for cross-linking, the hydrogels exhibited significantly lower storage moduli (1.36 kPa in 40 mM HEPES, 0.74 kPa in 0.5× DMEM, and 0.27 kPa in 1× PBS) compared to the one cross-linked in distilled water (3.1 kPa). Moreover, tyramine has been conjugated to SF (SF-TA) to allow HRP-mediated cross-linking. Using 40 mM HEPES as a buffer solution, the maximum storage modulus was ∼2.2 kPa for SF with 30% SF-TA compared to 1.4 kPa for SF-only hydrogels. As a result, the compressive modulus of composite hydrogels increased over time: in fact, at day 14, moduli of pristine SF and 10%, 30%, 50% SF-TA were above 45 kPa and reached 60−100 kPa at day 28 starting from 21.8 kPa at day 1.[132] SF could also be used in combination with other biomaterials to ameliorate hydrogel properties and to improve mechanical features. Although collagen is widely used for 3D culture because of its biocompatibility and biodegradability, it exhibits lower values of stiffness than natural tissues. A common and effective strategy to modulate the stiffness is to produce a collagen-silk hydrogel. Sanz-Fraile et al. reported the elastic modulus of collagen hydrogels at about 10 kPa, while silk-reinforced ones showed an increase in stiffness of more than 2-fold, reaching the maximum at 75% SF and 25% collagen (about 31 kPa).[133] The collagen component influenced cell adhesion rather than hydrogel stiffness and microstructure, which mainly depends on SF concentration. In fact, increasing SF concentration resulted in decreased porosity and rounded microstructure; this modulation was correlated to the changes in breast cancer cell morphology and invasion capability, underlining the importance of hydrogel structure in the study of cancer cell behavior.[134] Buitrago and colleagues observed that varying SF and collagen concentration, wide range of storage moduli may be obtained, i.e., from 0.017 kPa (at 0.35% SF + 0.5 mg/mL collagen) to 6.81 kPa (at 2.45% SF + 3.5 mg/mL collagen). In addition, the compressive modulus was estimated to be in the range 0.05−20.4 kPa. Human mesenchymal stem cells, encapsulated into these hydrogels, remained viable in long-term culture experiment.[135]

In another study, hydrogel stiffness was also modulated by changing the parameters of the preparation method, as the precise regulation of freezing temperature allowed the realization of hydrogels with different mechanical properties starting from the same SF solution and minimizing changes in roughness and porosity.[136] An alternative strategy was represented by the combination of tunable silk self-assembly properties and the traditional salt-leaching method. In this case, tuning the concentrating rates of silk solutions allowed to control nanoparticles sizes and so, through the salt-leaching process, the structure and the stiffness of the resulting hydrogel.[137] The use of SF nanofibers (SNF) was proposed as another way to obtain scaffolds with different mechanical properties.[138,139] Hydrogels derived from SNF having more tyrosine residues displayed four times higher stiffness than traditional SF solution, leading to a flattened morphology with better cytoskeleton development in bone marrow mesenchymal stem cells.[139]

5.3. GelMA. Gelatin methacrylamide (GelMA) is widely used as biomaterial for hydrogel production. Typically, GelMA is prepared by reacting gelatin with methacrylic anhydride, and then the hydrogel is obtained after photopolymerization. The degree of substitution, the temperature, and the photoinitiator concentration can influence the mechanical properties of the hydrogel because of the resulting extent of cross-linking.[140] GelMA demonstrated remarkable properties that allowed cell adhesion, migration, and proliferation and it could also be used for the realization of a microfluidic device, thanks to its high printing resolution.[141] Ha and colleagues observed that an elastic modulus of 7 kPa (10% GelMa) promoted dental stem cell proliferation, and no further increase in cell density was observed at higher stiffness. Thus, the precise control of mechanical features was fundamental to reach the ideal cell culture conditions.[142] Indeed, cell lineage specification is directed by mimicking the elasticity of the desired tissue.[143] In a similar manner, Lin et al. produced different hydrogels by changing the GelMA concentration, and their Young's modulus ranged from 25.59 to 41.78 kPa. They observed that bone marrow-derived stem cells differentiated into endothelial cells mainly in hydrogels with a lower and medium stiffness (25.59 and 33 kPa, respectively), suggesting that the fine regulation of mechanical properties could influence cell behavior.[144] Wu and colleagues proved that increasing GelMA concentration to 30% allowed to produce a hydrogel with an elastic modulus as high as 184.52 kPa.[145] Thanks to the fact that mechanical properties could be regulated by photo cross-linking, Kim et al. succeeded in producing a stiffness gradient into a GelMA hydrogel. Specifically, a UV photomask of 20−100% of transparency was used to polymerize 10% GelMA, obtaining a Young's modulus ranging from 3.5 to 13.1 kPa. When the photomask was substituted with the one with 10−100% transparency, the range changed from 5.4 to 18.5 kPa over the length. The hydrogel stiffness was able to drive the mesenchymal stem cell differentiation toward adipogenic or myogenic lineages. These effects are inhibited by blocking cell contractility using an actomyosin disrupting agent or an inhibitor of a kinase involved in this process. Hence, demonstrating that mechanotransdution is fundamental for cell survival and differentiation.[146]

GelMa has also been successfully combined with other biomaterials with the aim of enhancing the mechanical properties or for designing gels employed in specific studies. For example, to understand how normal osteoblast and osteosarcoma cells responded to different substrate stiffness, Jiang et al. produced a PEGDA/GelMA hydrogel in which GelMA concentration was responsible for the adhesive properties, and the introduction of PEGDA allowed the tuning of the mechanical features; the hydrogel modulus varied from 1.6 to 25 kPa with the increase of PEGDA concentration. Interestingly, they observed that osteosarcoma cell proliferation and tumorigenesis were enhanced in a stiffer hydrogel.

https://dx.doi.org/10.1021/acsabm.0c01472
ACS Appl. Bio Mater. 2021, 4, 2233−2250

Indeed, several tumorigenic markers (e.g., MMP9, MMP2, VEGF, and HIFA) were more expressed in the stiffer matrix, and the same trend was detected for markers linked to tumor invasion and metastasis; this is regulated by integrin-mediated signaling. Instead, osteoblasts showed a behavior more dependent on the adhesion ligands provided by GelMA than on stiffness.[147] Other studies demonstrated that a higher PEGDA and GelMA content was able to increase bone marrow-derived stem cell (BMSC) proliferation and promote chondrogenic commitment when compared with softer gels.[148] As well, Peter and colleagues observed that 5% GelMA had a storage modulus of 13 Pa, which could be increased by 30−150 Pa, adding PEGDA with various molecular weights and changing its concentration from 1% to 2%. In addition, when PEGDA concentration was increased to 7.5% or 15%, different moduli from 1 to 8 kPa were detected.[149]

Silk fibers have also been used to produce fiber-reinforced hydrogels as reported by Xiao and colleagues that added silk microfibers of different lengths to GelMA hydrogels. The introduction of silk significantly increased the stiffness proportionally to the fiber length but deteriorated, at the same time, the stability of the gel. The authors demonstrated that the cells were more prone to adhere and proliferate on composite hydrogels containing longer microfibers.[150]

5.4. Hyaluronic Acid. Hyaluronic acid (HA) is a glycosaminoglycan present in the extracellular environment of many tissues. It provides several advantages, including biodegradability, biocompatibility, and the presence of functional groups, which promote its use as a scaffold for 3D culture and tissue engineering. HA is a component of human ECM, and its role is fundamental in connective tissue, where it induces cell growth and differentiation. The presence of the carboxylic acid and hydroxyl groups allows cross-linking via ether or ester linkage or covalent modification to form other reactive motifs. Several approaches may be adopted to obtain 3D scaffold including electrospinning, freeze-drying, micropatterning, and phase separation.[151] For effective use of scaffolds, consistency properties are very important so that cells can regulate biological processes such as proliferation and migration based on the stiffness of the material. Furthermore, the rigidity of the scaffolds is also crucial for cell fate. Asim et al. succeeded in obtaining an S-protected thiolated HA that was used to produce a hydrogel with enhanced mechanical properties: *N*-acetyl cysteine (NAC) was linked to succinimidyl 3-(2-pyridyldithio) propionate (SPDP) via a disulfide bond. Then, a carbodiimide was used to activate −COOH groups of HA which subsequently reacted with SPDP-NAC through amide bond formation. The gelation process was performed via a thioldisulfide exchange reaction, in which the cysteine-rich glycoproteins contained in mucus were mixed with the S-protected thiolated HA to mimic the extracellular compartment. This approach strongly increased both the viscosity and the elastic modulus of the hydrogel, which displayed no cytotoxicity, and its higher stiffness promoted changes in cell morphology.[152] Another strategy was proposed by Aviv and colleagues that reported the formation of composite hydrogels to retain biocompatibility and to improve mechanical properties. The authors used a self-assembling peptide, fluorenylmethoxycarbonyl diphenylalanine (FmocFF), which was mixed with HA in different ratios to modulate stiffness. This approach shifted the hydrogel morphology from a symmetrical crystallization pattern of pure HA to a fibrous network, and its elastic modulus varied from 0.158 Pa to 20 kPa.[153] A thermoresponsive hydrogel with tunable mechanical and chemical properties was developed from HA and poly(*N*-isopropylacrylamide) (PNIPAAm) to support human pluripotent stem cells for *in vitro* expansion. Hydrogels that ranged from 0.5 to 4 kPa were obtained by modifying the molecular weight of the polymer, while variations of the polymer concentration allowed to increase the storage modulus due to the reduced distance between the chains. In particular, hydrogels obtained from 1 MDa HA-PNIPAAm and 1 MDa HA-P(NIPAAm-*r*-buthyl-methacrylate) at 7.,5% demonstrated to be suitable for human pluripotent stem cell viability and proliferation (storage moduli ≈ 1 kPa).[154] Kuss and colleagues designed a hydrogel that consisted of methacrylated HA and methacrylated gelatin; the authors were able to modulate the photo-cross-linking time in order to obtain different degrees of stiffness. Particularly, compressive modulus of a 30 s photo-cross-linked construct was 2.02 ± 1.11 kPa, whereas the modulus of a 90 s photo-cross-linked one was 9.17 ± 3.14 kPa. Human adipocytes progenitors were encapsulated into the bioink, which was then printed into disc-shaped constructs and porous ones with the help of predesigned lines. Then, the analysis of the induction of white adipocytes (WA) and brown adipocytes (BA) was performed to assess stiffness effects: BA were induced in stiff and porous constructs which showed a higher amount of Prdm16, a key regulator of their development, whereas WA were induced in soft and porous hydrogels.[155] In another interesting work, Duan and colleagues designed an *in vitro* system to mimic the vascularization process. A pH-responsive hydrogel was derived from methacrylated HA (HA-MA), periodate-oxidase HA (HA-ALH), and HA modified with adipic hydrazide (HA-ADH). First, a Schiff base hydrogel was formed from HA-ALH and HA-ADH, and then, the double network hydrogel was derived from the mixture of this base and HA-MA through UV-irradiation-based cross-linking. The elastic modulus of the hydrogel was significantly affected by pH and decreased from 15.77 to 4.8 kPa when it passed from physiological pH to pH 5. Migration assays showed that endothelial cells migrated deeper in the softer hydrogel, while mesenchymal stem cells had the opposite behavior.[156] Taken together, all these approaches revealed a high versatility of HA hydrogels with a plethora of parameters that could be tuned to improve mechanical properties but also to adapt the culture conditions to mimic real tissue composition. HA hydrogels have also been used for *in vitro* studies of cancer cell features. Narkhede and colleagues analyzed the behavior of a breast cancer cell line in a hydrogel formed by HA functionalized with methacrylate groups. The stiffness was strongly regulated by the concentration of the cross-linker dithiothreitol. The authors observed that cells acquired spread morphology in stiffer hydrogels, proliferating and migrating more as the hydrogel stiffness increased.[157] To study the effect of matrix composition and stiffness on the behavior of glioblastoma cells, Bonnesoeur et al. designed HA-hydrogels with different ECM components (poly-L-lysin, type III collagen, type IV collagen) cross-linked with genipin (GnP). GnP cross-linking increased HA-hydrogel stiffness from 0.1 kPa to almost 2 kPa. Regarding cell behavior, viability and proliferation were enhanced by a higher stiffness and by the addition of type IV collagen.[158] Another study conducted by Erickson et al. reported the development of HA-chitosan scaffolds with a different elastic modulus that ranged from 1.41 to 27.7 kPa and, consequently, with different density and porosity. The

https://dx.doi.org/10.1021/acsabm.0c01472
ACS Appl. Bio Mater. 2021, 4, 2233−2250

authors did not detect any difference in cell viability among different scaffolds whereas spheroids formation and expression of genes related to invasion and drug resistance were increased in stiffer scaffolds and cells were more resistant to a chemotherapeutic agent called Temozolomid.[80] Always in the framework of composite HA constructs, Xiao et al. developed a hydrogel for culture of patient-derived glioblastoma cells. HA was modified with thiol groups and then cross-linked via maleimide groups with polyethylene glycol (PEG), whose concentration changed the gel stiffness from 1 to 2 kPa. The authors compared the response of glioma cells derived from patients to a chemotherapeutic agent; the cells were cultured as gliomaspheres or within hydrogels that mimicked brain stiffness. Interestingly, in the latter case, cells acquired drug resistance, and hydrogels with higher HA content and 1 kPa stiffness induced more resistance compared to stiffer gels.[159] These works underlined the importance of stiffness regulation because glioblastoma cell proliferation and drug sensitivity are strongly influenced by the matrix where they grow. For instance, the development of an *in vitro* model that resembles the mechanical properties of native tissue could be helpful for the selection of drugs with potential therapeutic effects. Scaffold structure and architecture can also be controlled by the stiffness of the materials from which it is made. Hydrogel rigidity can consequently promote cell growth and survival within the 3D network of the scaffold. Furthermore, changes in rheological behavior can lead to a change in cell morphology, to allow for repair of damaged tissues, for example.

5.5. Peptide-Based Hydrogel. Peptide-based hydrogels are useful tools in the biomedical field for their high-water content, tunable mechanical properties, structure, stability, and biocompatibility. They are mainly used for drug delivery and 3D tissue culture, and many approaches may be used for obtaining hydrogels, including spontaneous, enzyme-controlled, or cross-linking-enhanced hydrogelation. Self-assembling is promoted by electrostatic interactions, hydrogen bonding, hydrophobic forces, and $\pi-\pi$ stacking, while enzymatic-driven hydrogelation shows advantages in terms of biocompatibility and finest control of the reaction.[160] Bairaghi and colleagues developed a hydrogel starting from L-histidine tripeptide, reinforced by the addition of different dicarboxylic acids. Precisely, succinic acid was able to stabilize the gel by increasing melting temperature and, importantly, to enhance stiffness reaching a storage modulus value of ≈9.7 kPa. Succinic acid also promoted the shifting from spherical morphology to the nanofibrous network structure, which mimics the extracellular matrix organization.[161] To further improve mechanical properties, peptides with an opposite charge on their residues may be used, as proposed by Jian and colleagues that used the two oppositely charged dipeptides Fmoc-tyrosine-lysine and Fmoc-tyrosine-aspartic acid. Depending on the starting peptide concentration, the storage modulus shifted from 4 to 62 kPa.[162] Another approach consisted of the self-assembly of peptides that established strong interactions with each other to improve mechanical properties. In particular, the EFK8 self-assembling peptide, which contains both hydrophilic (lysine and glutamic acid) and hydrophobic (phenylalanine) residues, was chosen because of its ability to establish hydrophobic, electrostatic, hydrogen bond, and van der Waals' forces mediated interactions and was used in the production of hydrogels for tissue engineering. The compressive modulus of the hydrogels varied from 44 to 104 Pa promoting morphological changes in cancer cells. The increased stiffness of the hydrogel leads to a change in the morphology of the cell line (A549) from spheroidal to elongated, which can be visually controlled. The possibility of modulating the rheological properties with self-assembling peptides or by incorporating a single-wall nanotube into their structure paves the way to the study of the microenvironment and cell adhesion in terms of invasiveness of tumor cells.[163] Ichise et al. developed a collagen-like peptide polymer with the main goal of realizing an environment that resembled *in vivo* ECM. Specifically, polymerization consisted in the formation of disulfide bonds among cysteine residues (Cys) present at both ends of the peptides; the number of Cys residues allowed to modulate the Young's modulus and produce gels with specific mechanical properties (40.6 ± 6.2 kPa, 671 ± 67 kPa, and 709 ± 63 kPa). Finally, the incorporation of the binding sequence for the integrin $\alpha2\beta1$ promoted cell adhesion.[164] A similar strategy is represented by the use of modified amphiphilic peptides to allow self-assembly through host−guest interactions.[165] Covalent incorporation of β-cyclodextrin (host) or adamantane (guest) to peptide amphiphiles leads to the formation of hydrogels whose mechanical properties may be precisely controlled. In fact, by changing the ratio between host and guest molecules, Redondo-Gomez and colleagues obtained gels with the storage modulus that ranged from 2.8 ± 0.5 kPa to 5.1 ± 0.8 kPa. By using supramolecular hydrogels, it is possible to remedy the traditional approaches to regulate the stiffness of the material, which by modifying its concentration or cross-linking density, leads to a concomitant change in the characteristics of the scaffold. Thanks to the presence of dynamic bonds, supramolecular hydrogels make it possible to modulate stiffness selectively without affecting other parameters of the hydrogel. such as bioactivity or degradation[166]

5.6. PEG-Based Materials. Poly(ethylene glycol) orPEG is an hydrophilic polymer used for biomedical applications (e.g., drug delivery, 3D scaffold) for its biocompatibility and absence of immunogenicity. Its two hydroxyl groups may be converted into several functional motifs (e.g., acrylate, azide, thiol, amine), which can be used to form the hydrogel. Further, to better simulate natural ECM, PEG can be modified to contain cell adhesive peptide (e.g., RGD) or growth factor to allow cell adhesion and control proliferation, differentiation and migration.[167] PEG has been used for designing gels with a wide range of stiffness values. Crocini et al. reported the realization of PEG hydrogels by thiol−ene reaction using PEG norbornene, PEG thiol (PEG-SH), and lithium phenyl-2,4,6-trimethylbenzoylphosphinate (LAP) as a photoinitiator in the photopolymerization reaction. Stiffness was modulated by varying PEG-SH during the polymerization, and it could be changed dynamically by putting the gels into stiffening solution, which consisted of the two PEG types and LAP. Although no differences were detected in cardiomyocyte viability among different gels, contractility and localization of a mechanosensitive transcription factor called Yes-associated protein (YAP) were influenced by stiffness.[168] A remarkable application of host−guest interaction was proposed by Shih and colleagues, who designed a gel that was the result of a light-mediated thiol-allylether click reaction between thiolated poly(vinyl alcohol) (TPVA), 4-arm poly(ethylene glycol)-allylether (PEG4AE), and β-cyclodextrin-allylether (βCDAE) as host moiety. Providing 4-arm PEG-adamantane (PEG4AD), which acted as a guest, cross-linking and elastic modulus were

https://dx.doi.org/10.1021/acsabm.0c01472
ACS Appl. Bio Mater. 2021, 4, 2233−2250

increased from 2.3 to 6.5 kPa. This approach also allowed softening of the material by adding β-cyclodextrin due to the competitive binding with the guest present into the hydrogel. The proposed material was a dynamic hydrogel with matrix stiffness tunable on demand. The change in the stiffness of the material is completely reversible and can be activated on request. These hydrogels are ideal for studies on the effect of matrix mechanics on cell fate processes.[169]

5.7. Dextran-Based Materials. Dextran is a biocompatible polysaccharide characterized by low protein adsorption and high hydrophilicity. The presence of many hydroxyl groups allowed the functionalization with chemical groups (e.g., vinyl sulfone or methacrylation) to promote hydrogel formation or with peptide (e.g., RGD) to enhance cell attachment. Further, the possibility to obtain different degrees of substitution enabled the designing of hydrogels with various levels of stiffness.[170−172]

In this context, Kim and colleagues embedded induced hepatic progenitor cells (iHEPs) into a hydrogel made of methacrylic gelatin (GelMA) and methacrylic dextran (DeMA). Specifically, gels were designed with different percentages of GelMA (from 6 wt % to 10 wt %) and 1 wt % of DeMA at different degrees of substitution. Thus, the addition of DeMA with higher levels of substitution resulted in higher compressive modulus compared to GelMA hydrogels without changing the number of cell adhesion sites. Further, the presence of DeMA sustained cell migration and cell−cell junction formation, demonstrating that dextran ameliorated GelMA hydrogel features.[173] Dextran vinyl sulfone derived from the reaction between dextran and divinyl sulfone was used for the synthesis of a mechanically stable fibrous matrix. Young's modulus depended on the time of photopolymerization and concentration of the photoinitiator. Specifically, Davidson and colleagues were able to adjust the modulus from 0.77 to 11.03 kPa, and the functionalization with RGD promoted adhesion and spreading of normal human lung fibroblasts.[174]

6. CONCLUSIONS AND PERSPECTIVES

In summary, we reviewed recent developments regarding the synthesis and modification of soft materials that can be used to mimic the mechanical properties of real tissue, thereby serving as an ideal and tunable 3D matrix. Despite the progress already made, the challenges remain in getting closer to real matrix and tissue and reproducibility between experiments. First, the theory currently goes far beyond the experiment and feedback from experiment to theoretical modeling is sorely lacking. A possible improvement could be to follow the latest trends that seek to combine image analyzes in context with rheological analyses (e.g., confocal rheometry). In this way, very detailed information could be found with respect to the mechanistic understanding of the deformation of soft materials. This could be a good starting point for the development of theoretical models and suggest new technological applications. Second, for their best applications, it would be necessary to understand the key parameter of mechanotransduction, deeply connected to cell behavior under different mechanical stress stimuli. Therefore, both experiment and theory efforts are needed to accelerate the development of research and applications of 3D culture reproduction.

AUTHOR INFORMATION

Corresponding Author

Francesca Frascella − *Dipartimento di Scienza Applicata e Tecnologia and PolitoBIOMed Lab, Politecnico di Torino, Turin 10129, Italy;* orcid.org/0000-0002-6543-6038; Email: francesca.frascella@polito.it

Authors

Désirée Baruffaldi − *Dipartimento di Scienza Applicata e Tecnologia and PolitoBIOMed Lab, Politecnico di Torino, Turin 10129, Italy*

Gianluca Palmara − *Dipartimento di Scienza Applicata e Tecnologia and PolitoBIOMed Lab, Politecnico di Torino, Turin 10129, Italy*

Candido Pirri − *Dipartimento di Scienza Applicata e Tecnologia and PolitoBIOMed Lab, Politecnico di Torino, Turin 10129, Italy; Center for Sustainable Futures@Polito, Istituto Italiano di Tecnologia, Turin 10144, Italy*

Complete contact information is available at: https://pubs.acs.org/10.1021/acsabm.0c01472

Author Contributions

The manuscript was written through contributions of all authors. All authors have given approval to the final version of the manuscript.

Funding

The present work was performed in the framework of POLITO BIO Med LAB, an interdepartmental laboratory financed by Politecnico di Torino, DEFLeCT, and Food Drug Free projects funded by Regione Piemonte POR-FESR 2014−2020.

Notes

The authors declare no competing financial interest.

REFERENCES

(1) Griffith, L. G.; Swartz, M. A. Capturing Complex 3D Tissue Physiology in Vitro. *Nat. Rev. Mol. Cell Biol.* **2006**, *7* (3), 211−224.

(2) Bleu Knight, V.; Serrano, E. E. Hydrogel Scaffolds Promote Neural Gene Expression and Structural Reorganization in Human Astrocyte Cultures. *PeerJ.* **2017**, *2017* (1), 1.

(3) Fontoura, J. C.; Viezzer, C.; dos Santos, F. G.; Ligabue, R. A.; Weinlich, R.; Puga, R. D.; Antonow, D.; Severino, P.; Bonorino, C. Comparison of 2D and 3D Cell Culture Models for Cell Growth, Gene Expression and Drug Resistance. *Mater. Sci. Eng., C* **2020**, *107*, 110264.

(4) Ma, L.; Zhang, B.; Zhou, C.; Li, Y.; Li, B.; Yu, M.; Luo, Y.; Gao, L.; Zhang, D.; Xue, Q.; Qiu, Q.; Lin, B.; Zou, J.; Yang, H. The Comparison Genomics Analysis with Glioblastoma Multiforme (GBM) Cells under 3D and 2D Cell Culture Conditions. *Colloids Surf., B* **2018**, *172* (July), 665−673.

(5) Joyce, J. A.; Pollard, J. W. Microenvironmental Regulation of Metastasis. *Nat. Rev. Cancer* **2009**, *9* (4), 239−252.

(6) Hoarau-Véchot, J.; Rafii, A.; Touboul, C.; Pasquier, J. Halfway between 2D and Animal Models: Are 3D Cultures the Ideal Tool to Study Cancer-Microenvironment Interactions? *Int. J. Mol. Sci.* **2018**, *19* (1), 181.

(7) Trédan, O.; Galmarini, C. M.; Patel, K.; Tannock, I. F. Drug Resistance and the Solid Tumor Microenvironment. *J. Natl. Cancer Inst.* **2007**, *99* (19), 1441−1454.

(8) Wang, K.; Kievit, F. M.; Erickson, A. E.; Silber, J. R.; Ellenbogen, R. G.; Zhang, M. Culture on 3D Chitosan-Hyaluronic Acid Scaffolds Enhances Stem Cell Marker Expression and Drug Resistance in Human Glioblastoma Cancer Stem Cells. *Adv. Healthcare Mater.* **2016**, *5* (24), 3173−3181.

(9) Brancato, V.; Oliveira, J. M.; Correlo, V. M.; Reis, R. L.; Kundu, S. C. Could 3D Models of Cancer Enhance Drug Screening? *Biomaterials* **2020**, *232*, 119744.
(10) Chaicharoenaudomrung, N.; Kunhorm, P.; Promjantuek, W.; Heebkaew, N.; Rujanapun, N.; Noisa, P. Fabrication of 3D Calcium-Alginate Scaffolds for Human Glioblastoma Modeling and Anticancer Drug Response Evaluation. *J. Cell. Physiol.* **2019**, *234* (11), 20085−20097.
(11) Goldmann, W. H. *Mechanosensation: A Basic Cellular Process* **2014**, *126*, 1.
(12) Kechagia, J. Z.; Ivaska, J.; Roca-Cusachs, P. Integrins as Biomechanical Sensors of the Microenvironment. *Nat. Rev. Mol. Cell Biol.* **2019**, *20* (8), 457−473.
(13) Nemec, S.; Kilian, K. A. Materials Control of the Epigenetics Underlying Cell Plasticity. *Nat. Rev. Mater.* **2021**, *6*, 69.
(14) Romani, P.; Valcarcel-Jimenez, L.; Frezza, C.; Dupont, S. Crosstalk between Mechanotransduction and Metabolism. *Nat. Rev. Mol. Cell Biol.* **2021**, *22*, 22−38.
(15) Wang, C.; Sinha, S.; Jiang, X.; Murphy, L.; Fitch, S.; Wilson, C.; Grant, G.; Yang, F. Matrix Stiffness Modulates Patient-Derived Glioblastoma Cell Fates in 3D Hydrogels. *Tissue Eng., Part A* **2020**, 1−33.
(16) Zhu, D.; Tong, X.; Trinh, P.; Yang, F. Mimicking Cartilage Tissue Zonal Organization by Engineering Tissue-Scale Gradient Hydrogels as 3D Cell Niche. *Tissue Eng., Part A* **2018**, *24* (1−2), 1−10.
(17) Sacchi, M.; Bansal, R.; Rouwkema, J. Bioengineered 3D Models to Recapitulate Tissue Fibrosis. *Trends Biotechnol.* **2020**, *38* (6), 623−636.
(18) Lam, C. R. I.; Wong, H. K.; Nai, S.; Chua, C. K.; Tan, N. S.; Tan, L. P. A 3D Biomimetic Model of Tissue Stiffness Interface for Cancer Drug Testing. *Mol. Pharmaceutics* **2014**, *11* (7), 2016−2021.
(19) Acerbi, I.; Cassereau, L.; Dean, I.; Shi, Q.; Au, A.; Park, C.; Chen, Y. Y.; Liphardt, J.; Hwang, E. S.; Weaver, V. M. Human Breast Cancer Invasion and Aggression Correlates with ECM Stiffening and Immune Cell Infiltration. *Integr. Biol. (United Kingdom)* **2015**, *7* (10), 1120−1134.
(20) Chang, J. M.; Park, I. A.; Lee, S. H.; Kim, W. H.; Bae, M. S.; Koo, H. R.; Yi, A.; Kim, S. J.; Cho, N.; Moon, W. K. Stiffness of Tumours Measured by Shear-Wave Elastography Correlated with Subtypes of Breast Cancer. *Eur. Radiol.* **2013**, *23* (9), 2450−2458.
(21) McIlvain, G.; Schwarb, H.; Cohen, N. J.; Telzer, E. H.; Johnson, C. L. Mechanical Properties of the in Vivo Adolescent Human Brain. *Dev. Cogn. Neurosci.* **2018**, *34* (June), 27−33.
(22) Zhang, Y.; Zhang, F.; Yan, Z.; Ma, Q.; Li, X.; Huang, Y.; Rogers, J. A. Printing, Folding and Assembly Methods for Forming 3D Mesostructures in Advanced Materials. *Nat. Rev. Mater.* **2017**, *2* (4), 1.
(23) Deforest, C. A.; Tirrell, D. A. A Photoreversible Protein-Patterning Approach for Guiding Stem Cell Fate in Three-Dimensional Gels. *Nat. Mater.* **2015**, *14* (5), 523−531.
(24) Yilmaz, C. O.; Xu, Z. S.; Gracias, D. H. *Curved and Folded Micropatterns in 3D Cell Culture and Tissue Engineering* **2014**, *121*, 1.
(25) Tan, Y.; Hu, B.; Song, J.; Chu, Z.; Wu, W. *Bioinspired Multiscale Wrinkling Patterns on Curved Substrates: An Overview* **2020**, *12*, 1.
(26) Ning, X.; Wang, X.; Zhang, Y.; Yu, X.; Choi, D.; Zheng, N.; Kim, D. S.; Huang, Y.; Zhang, Y.; Rogers, J. A. Assembly of Advanced Materials into 3D Functional Structures by Methods Inspired by Origami and Kirigami: A Review. *Adv. Mater. Interfaces* **2018**, *5* (13), 1−13.
(27) Bolaños Quiñones, V. A.; Zhu, H.; Solovev, A. A.; Mei, Y.; Gracias, D. H. Origami Biosystems: 3D Assembly Methods for Biomedical Applications. *Adv. Biosyst.* **2018**, *2* (12), 1−18.
(28) Hilderbrand, A. M.; Ovadia, E. M.; Rehmann, M. S.; Kharkar, P. M.; Guo, C.; Kloxin, A. M. Biomaterials for 4D Stem Cell Culture. *Curr. Opin. Solid State Mater. Sci.* **2016**, *20* (4), 212−224.
(29) Zheng, Y.; Liong Han, M. K.; Jiang, Q.; Li, B.; Feng, J.; Del Campo, A. 4D Hydrogel for Dynamic Cell Culture with Orthogonal, Wavelength-Dependent Mechanical and Biochemical Cues. *Mater. Horiz.* **2020**, *7* (1), 111−116.
(30) Miao, S.; Cui, H.; Esworthy, T.; Mahadik, B.; Lee, S. jun; Zhou, X.; Hann, S. Y.; Fisher, J. P.; Zhang, L. G. 4D Self-Morphing Culture Substrate for Modulating Cell Differentiation. *Adv. Sci.* **2020**, *7* (6), 1902403.
(31) Palmara, G.; Frascella, F.; Roppolo, I.; Chiappone, A.; Chiadò, A. Functional 3D Printing: Approaches and Bioapplications. *Biosens. Bioelectron.* **2021**, *175*, 112849.
(32) Ophir, J.; Ponnekanti, H.; Cespedes, I.; Yazdi, Y. X. L. Elastography: A Method for Imaging the Elasticity in Biological Tissues. *Ultrason. Imaging* **1991**, *13* (2), 111−134.
(33) Kennedy, B. F.; Wijesinghe, P.; Sampson, D. D. The Emergence of Optical Elastography in Biomedicine. *Nat. Photonics* **2017**, *11* (4), 215−221.
(34) Sigrist, R. M. S.; Liau, J.; Kaffas, A. El; Chammas, M. C.; Willmann, J. K. Ultrasound Elastography: Review of Techniques and Clinical Applications. *Theranostics* **2017**, *7* (5), 1303−1329.
(35) Shiina, T.; Nightingale, K. R.; Palmeri, M. L.; Hall, T. J.; Bamber, J. C.; Barr, R. G.; Castera, L.; Choi, B. I.; Chou, Y. H.; Cosgrove, D.; Dietrich, C. F.; Ding, H.; Amy, D.; Farrokh, A.; Ferraioli, G.; Filice, C.; Friedrich-Rust, M.; Nakashima, K.; Schafer, F.; Sporea, I.; Suzuki, S.; Wilson, S.; Kudo, M. WFUMB Guidelines and Recommendations for Clinical Use of Ultrasound Elastography: Part 1: Basic Principles and Terminology. *Ultrasound Med. Biol.* **2015**, *41* (5), 1126−1147.
(36) Papadacci, C.; Bunting, E. A. 3D Quasi-Static Ultrasound Elastography With Plane Wave In Vivo. *IEEE Trans Med. Imaging* **2017**, *36* (2), 357−365.
(37) Hendriks, G. A G M; Hollander, B.; Menssen, J.; Milkowski, A.; Hansen, H. H G; de Korte, C. L Automated 3D Ultrasound Elastography of the Breast: A Phantom Validation Study. *Phys. Med. Biol.* **2016**, *61* (7), 2665−2679.
(38) Sathiyamoorthy, S. Towards Quantitative Quasi-Static Ultrasound Elastography Using a Reference Layer for Liver Imaging Application: A Preliminary Assessment. *Ultrasonics* **2019**, *93*, 7−17.
(39) Reiter, R.; Majumdar, S.; Kearney, S.; Kajdacsy-Balla, A.; Macias, V.; Crivellaro, S.; Caldwell, B.; Abern, M.; Royston, T. J.; Klatt, D. Prostate Cancer Assessment Using MR Elastography of Fresh Prostatectomy Specimens at 9.4 T. *Magn. Reson. Med.* **2020**, *84* (1), 396−404.
(40) Loomba, R.; Cui, J.; Wolfson, T.; Haufe, W.; Hooker, J.; Szeverenyi, N.; Ang, B.; Bhatt, A.; Wang, K.; Aryafar, H.; Behling, C.; Valasek, M. A.; Lin, G. Y.; Gamst, A.; Brenner, D. A.; Yin, M.; Glaser, K. J.; Ehman, R. L.; Sirlin, C. B. Novel 3D Magnetic Resonance Elastography for the Noninvasive Diagnosis of Advanced Fibrosis in NAFLD: A Prospective Study. *Am. J. Gastroenterol.* **2016**, *111* (7), 986−994.
(41) Mariappan, Y. K.; Glaser, K. J.; Ehman, R. L. Magnetic Resonance Elastography: A Review. *Clin Anat.* **2010**, *23* (5), 497−511.
(42) Sandrin, L.; Fourquet, B.; Hasquenoph, J. M.; Yon, S.; Fournier, C.; Mal, F.; Christidis, C.; Ziol, M.; Poulet, B.; Kazemi, F.; Beaugrand, M.; Palau, R. Transient Elastography: A New Noninvasive Method for Assessment of Hepatic Fibrosis. *Ultrasound Med. Biol.* **2003**, *29* (12), 1705−1713.
(43) Rouvière, O.; Melodelima, C.; Hoang Dinh, A.; Bratan, F.; Pagnoux, G.; Sanzalone, T.; Crouzet, S.; Colombel, M.; Mège-Lechevallier, F.; Souchon, R. Stiffness of Benign and Malignant Prostate Tissue Measured by Shear-Wave Elastography: A Preliminary Study. *Eur. Radiol.* **2017**, *27* (5), 1858−1866.
(44) de Lédinghen, V.; Vergniol, J. Transient Elastography (FibroScan). *Gastroenterol. Clin. Biol.* **2008**, *32* (6), 58−67.
(45) Sarvazyan, A.; J. Hall, T.; W. Urban, M.; Fatemi, M.; R. Aglyamov, S.; S. Garra, B. An Overview of Elasticity Imaging - an Emerging Branch of Medical Imaging. *Curr. Med. Imaging Rev.* **2011**, *7* (4), 255−282.
(46) Payen, T.; Oberstein, P. E.; Saharkhiz, N.; Palermo, C. F.; Sastra, S. A.; Han, Y.; Nabavizadeh, A.; Sagalovskiy, I. R.; Orelli, B.;

https://dx.doi.org/10.1021/acsabm.0c01472
ACS Appl. Bio Mater. 2021, 4, 2233−2250

Rosario, V.; Desrouilleres, D.; Remotti, H.; Kluger, M. D.; Schrope, B. A.; Chabot, J. A.; Iuga, A. C.; Konofagou, E. E.; Olive, K. P. Harmonic Motion Imaging of Pancreatic Tumor Stiffness Indicates Disease State and Treatment Response. *Clin. Cancer Res.* **2020**, *26* (6), 1297−1308.
(47) Konofagou, E. E.; Hynynen, K. H. Harmonic Motion Imaging: A New Technique for the Detection of the Local Mechanical Properties of Tissues. *Proc. SPIE* **2003**, *5035* (2003), 242.
(48) Hsu, C.; Caussy, C.; Imajo, K.; Chen, J.; Singh, S.; Kaulback, K.; Le, M. Da; Hooker, J.; Tu, X.; Bettencourt, R.; Yin, M.; Sirlin, C. B.; Ehman, R. L.; Nakajima, A.; Loomba, R. Magnetic Resonance vs Transient Elastography Analysis of Patients With Nonalcoholic Fatty Liver Disease: A Systematic Review and Pooled Analysis of Individual Participants. *Clin. Gastroenterol. Hepatol.* **2019**, *17* (4), 630−637.
(49) Imajo, K.; Kessoku, T.; Honda, Y.; Tomeno, W.; Ogawa, Y.; Mawatari, H.; Fujita, K.; Yoneda, M.; Taguri, M.; Hyogo, H.; Sumida, Y.; Ono, M.; Eguchi, Y.; Inoue, T.; Yamanaka, T.; Wada, K.; Saito, S.; Nakajima, A. Magnetic Resonance Imaging More Accurately Classifies Steatosis and Fibrosis in Patients with Nonalcoholic Fatty Liver Disease Than Transient Elastography. *Gastroenterology* **2016**, *150* (3), 626−637.
(50) Park, C. C.; Nguyen, P.; Hernandez, C.; Bettencourt, R.; Ramirez, K.; Fortney, L.; Hooker, J.; Sy, E.; Savides, M. T.; Alquiraish, M. H.; Valasek, M. A.; Rizo, E.; Richards, L.; Brenner, D.; Sirlin, C. B.; Loomba, R. Magnetic Resonance Elastography vs Transient Elastography in Detection of Fibrosis and Noninvasive Measurement of Steatosis in Patients With Biopsy-Proven Nonalcoholic Fatty Liver Disease. *Gastroenterology* **2017**, *152* (3), 598−607.
(51) O'Hara, S.; Hodson, S.; Hernaman, C.; Wambeek, N.; Olynyk, J. Concordance of Transient Elastography and Shear Wave Elastography for Measurement of Liver Stiffness. *Sonography* **2017**, *4* (4), 141−145.
(52) Butcher, D. T.; Alliston, T.; Weaver, V. M. A Tense Situation: Forcing Tumour Progression. *Nat. Rev. Cancer* **2009**, *9* (2), 108−122.
(53) Wang, L.; Wang, C.; Wu, S.; Fan, Y.; Li, X. *Biomater. Sci.* **2020**, *8*, 2714.
(54) d'Angelo, M.; Benedetti, E.; Tupone, M. G.; Catanesi, M.; Castelli, V.; Antonosante, A.; Cimini, A. The Role of Stiffness in Cell Reprogramming: A Potential Role for Biomaterials in Inducing Tissue Regeneration. *Cells* **2019**, *8* (9), 1036.
(55) Naqvi, S. M.; McNamara, L. M. Stem Cell Mechanobiology and the Role of Biomaterials in Governing Mechanotransduction and Matrix Production for Tissue Regeneration. *Front. Bioeng. Biotechnol.* **2020**, *8*, 1−27.
(56) Takata, K.; Goto, T.; Kuroda, M.; Kimura, Y.; Harada, I.; Ueda, K.; Kawada, T.; Kioka, N. Stiffness of the Extracellular Matrix Regulates Differentiation into Beige Adipocytes. *Biochem. Biophys. Res. Commun.* **2020**, *532* (2), 205−210.
(57) Zonderland, J.; Moroni, L. Steering Cell Behavior through Mechanobiology in 3D: A Regenerative Medicine Perspective. *Biomaterials* **2021**, *268*, 120572.
(58) Liu, Y.; Li, J.; Yao, B.; Wang, Y.; Wang, R.; Yang, S.; Li, Z.; Zhang, Y.; Huang, S.; Fu, X. The Stiffness of Hydrogel-Based Bioink Impacts Mesenchymal Stem Cells Differentiation toward Sweat Glands in 3D-Bioprinted Matrix. *Mater. Sci. Eng., C* **2021**, *118*, 111387.
(59) James, B. D.; Allen, J. B. Vascular Endothelial Cell Behavior in Complex Mechanical Microenvironments. *ACS Biomater. Sci. Eng.* **2018**, *4* (11), 3818−3842.
(60) Hu, M.; Jia, F.; Huang, W. P.; Li, X.; Hu, D. F.; Wang, J.; Ren, K. F.; Fu, G. S.; Wang, Y. B.; Ji, J. Substrate Stiffness Differentially Impacts Autophagy of Endothelial Cells and Smooth Muscle Cells. *Bioact. Mater.* **2021**, *6* (5), 1413−1422.
(61) Deng, Z.; Fear, M. W.; Suk Choi, Y.; Wood, F. M.; Allahham, A.; Mutsaers, S. E.; Prêle, C. M. The Extracellular Matrix and Mechanotransduction in Pulmonary Fibrosis. *Int. J. Biochem. Cell Biol.* **2020**, *126* (July), 105802.
(62) Singh, S.; Fujii, L. L.; Murad, M. H.; Wang, Z.; Asrani, S. K.; Ehman, R. L.; Kamath, P. S.; Talwalkar, J. A. Liver Stiffness Is Associated With Risk of Decompensation, Liver Cancer, and Death in Patients With Chronic Liver Diseases: A Systematic Review and Meta-Analysis. *Clin. Gastroenterol. Hepatol.* **2013**, *11* (12), 1573−e89.
(63) Mueller, S. Liver Stiffness: A Novel Parameter for the Diagnosis of Liver Disease. *Hepatic Med.* **2010**, 49.
(64) Insua-Rodríguez, J.; Oskarsson, T. The Extracellular Matrix in Breast Cancer. *Adv. Drug Delivery Rev.* **2016**, *97*, 41−55.
(65) Paszek, M. J.; Zahir, N.; Johnson, K. R.; Lakins, J. N.; Rozenberg, G. I.; Gefen, A.; Reinhart-King, C. A.; Margulies, S. S.; Dembo, M.; Boettiger, D.; Hammer, D. A.; Weaver, V. M. Tensional Homeostasis and the Malignant Phenotype. *Cancer Cell* **2005**, *8*, 241−254.
(66) Boyd, N. F.; Li, Q.; Melnichouk, O.; Huszti, E.; Martin, L. J.; Gunasekara, A.; Mawdsley, G.; Yaffe, M. J.; Minkin, S. Evidence That Breast Tissue Stiffness Is Associated with Risk of Breast Cancer. *PLoS One* **2014**, *9* (7), 1−8.
(67) Taubenberger, A. V.; Girardo, S.; Träber, N.; Fischer-Friedrich, E.; Kräter, M.; Wagner, K.; Kurth, T.; Richter, I.; Haller, B.; Binner, M.; Hahn, D.; Freudenberg, U.; Werner, C.; Guck, J. 3D Microenvironment Stiffness Regulates Tumor Spheroid Growth and Mechanics via P21 and ROCK. *Adv. Biosyst.* **2019**, *3* (9), 1−46.
(68) Khavari, A.; Nydén, M.; Weitz, D. A.; Ehrlicher, A. J. Composite Alginate Gels for Tunable Cellular Microenvironment Mechanics. *Sci. Rep.* **2016**, *6*, 1−11.
(69) Jiang, T.; Munguia-Lopez, J. G.; Gu, K.; Bavoux, M. M.; Flores-Torres, S.; Kort-Mascort, J.; Grant, J.; Vijayakumar, S.; De Leon-Rodriguez, A.; Ehrlicher, A. J.; Kinsella, J. M. Engineering Bioprintable Alginate/Gelatin Composite Hydrogels with Tunable Mechanical and Cell Adhesive Properties to Modulate Tumor Spheroid Growth Kinetics. *Biofabrication* **2020**, *12* (1), 015024.
(70) Cavo, M.; Fato, M.; Peñuela, L.; Beltrame, F.; Raiteri, R.; Scaglione, S. Microenvironment Complexity and Matrix Stiffness Regulate Breast Cancer Cell Activity in a 3D in Vitro Model. *Sci. Rep.* **2016**, *6* (October), 1−13.
(71) Yue, X.; Nguyen, T. D.; Zellmer, V.; Zhang, S.; Zorlutuna, P. Stromal Cell-Laden 3D Hydrogel Microwell Arrays as Tumor Microenvironment Model for Studying Stiffness Dependent Stromal Cell-Cancer Interactions. *Biomaterials* **2018**, *170*, 37−48.
(72) Hunter Joyce, M.; Lu, C.; James, E. R.; Hegab, R.; Allen, S. C.; Suggs, L. J.; Brock, A. Phenotypic Basis for Matrix Stiffness-Dependent Chemoresistance of Breast Cancer Cells to Doxorubicin. *Front. Oncol.* **2018**, *8* (SEP), 1−9.
(73) Rape, A.; Ananthanarayanan, B.; Kumar, S. Engineering Strategies to Mimic the Glioblastoma Microenvironment. *Adv. Drug Delivery Rev.* **2014**, *79*, 172−183.
(74) Chauvet, D.; Imbault, M.; Capelle, L.; Demene, C.; Mossad, M.; Karachi, C.; Boch, A. L.; Gennisson, J. L.; Tanter, M. In Vivo Measurement of Brain Tumor Elasticity Using Intraoperative Shear Wave Elastography. *Ultraschall der Medizin* **2016**, *37* (6), 584−590.
(75) Tabet, A.; Mommer, S.; Vigil, J. A.; Hallou, C.; Bulstrode, H.; Scherman, O. A. Mechanical Characterization of Human Brain Tissue and Soft Dynamic Gels Exhibiting Electromechanical Neuro-Mimicry. *Adv. Healthc. Mater.* **2019**, *8* (10), 1−5.
(76) Chen, X.; Wanggou, S.; Bodalia, A.; Zhu, M.; Dong, W.; Fan, J. J.; Yin, W. C.; Min, H. K.; Hu, M.; Draghici, D.; Dou, W.; Li, F.; Coutinho, F. J.; Whetstone, H.; Kushida, M. M.; Dirks, P. B.; Song, Y.; Hui, C. chung; Sun, Y.; Wang, L. Y.; Li, X.; Huang, X. A Feedforward Mechanism Mediated by Mechanosensitive Ion Channel PIEZO1 and Tissue Mechanics Promotes Glioma Aggression. *Neuron* **2018**, *100* (4), 799−815 e7.
(77) Kim, Y.; Kumar, S. CD44-Mediated Adhesion to Hyaluronic Acid Contributes to Mechanosensing and Invasive Motility. *Mol. Cancer Res.* **2014**, *12* (10), 1416−1429.
(78) Umesh, V.; Rape, A. D.; Ulrich, T. A.; Kumar, S. Microenvironmental Stiffness Enhances Glioma Cell Proliferation by Stimulating Epidermal Growth Factor Receptor Signaling. *PLoS One* **2014**, *9* (7), 1−8.
(79) Wang, C.; Tong, X.; Yang, F. Bioengineered 3D Brain Tumor Model to Elucidate the Effects of Matrix Stiffness on Glioblastoma

https://dx.doi.org/10.1021/acsabm.0c01472
ACS Appl. Bio Mater. 2021, 4, 2233−2250

Cell Behavior Using Peg-Based Hydrogels. *Mol. Pharmaceutics* **2014**, *11* (7), 2115−2125.
(80) Erickson, A. E.; Lan Levengood, S. K.; Sun, J.; Chang, F. C.; Zhang, M. Fabrication and Characterization of Chitosan−Hyaluronic Acid Scaffolds with Varying Stiffness for Glioblastoma Cell Culture. *Adv. Healthc. Mater.* **2018**, *7* (15), 1−9.
(81) Burgstaller, G.; Oehrle, B.; Gerckens, M.; White, E. S.; Schiller, H. B.; Eickelberg, O. The Instructive Extracellular Matrix of the Lung: Basic Composition and Alterations in Chronic Lung Disease. *Eur. Respir. J.* **2017**, *50* (1), 1601805.
(82) Angel, P. M.; Bruner, E.; Bethard, J.; Clift, C. L.; Ball, L.; Drake, R. R.; Feghali-Bostwick, C. Extracellular Matrix Alterations in Low-Grade Lung Adenocarcinoma Compared with Normal Lung Tissue by Imaging Mass Spectrometry. *J. Mass Spectrom.* **2020**, *55* (4), 0−2.
(83) Fakhouri, F.; Dong, H.; Kolipaka, A. Magnetic Resonance Elastography of the Lungs: A Repeatability and Reproducibility Study. *NMR Biomed.* **2019**, *32* (7), 1−10.
(84) Brown, A. C; Fiore, V. F; Sulchek, T. A; Barker, T. H Physical and Chemical Microenvironmental Cues Orthogonally Control the Degree and Duration of Fibrosis-Associated Epithelial-to-Mesenchymal Transitions. *J. Pathol* **2013**, *229* (1), 25−35.
(85) Liu, F.; Tschumperlin, D. J. Micro-Mechanical Characterization of Lung Tissue Using Atomic Force Microscopy. *J. Visualized Exp.* **2011**, No. 54, 1−7.
(86) Yuan, Y.; Zhong, W.; Ma, G.; Zhang, B.; Tian, H. Yes-Associated Protein Regulates the Growth of Human Non-Small Cell Lung Cancer in Response to Matrix Stiffness. *Mol. Med. Rep.* **2015**, *11* (6), 4267−4272.
(87) Shukla, V. C.; Higuita-Castro, N.; Nana-Sinkam, P.; Ghadiali, S. N. Substrate Stiffness Modulates Lung Cancer Cell Migration but Not Epithelial to Mesenchymal Transition. *J. Biomed. Mater. Res., Part A* **2016**, *104* (5), 1182−1193.
(88) Anguiano, M.; Morales, X.; Castilla, C.; Pena, A. R.; Ederra, C.; Martínez, M.; Ariz, M.; Esparza, M.; Amaveda, H.; Mora, M.; Movilla, N.; García Aznar, J. M.; Cortés-Domínguez, I.; Ortiz-De-Solorzano, C. The Use of Mixed Collagen-Matrigel Matrices of Increasing Complexity Recapitulates the Biphasic Role of Cell Adhesion in Cancer Cell Migration: ECM Sensing, Remodeling and Forces at the Leading Edge of Cancer Invasion. *PLoS One* **2020**, *15* (1), 1−29.
(89) Vigier, S.; Gagnon, H.; Bourgade, K.; Klarskov, K.; Fülöp, T.; Vermette, P. Composition and Organization of the Pancreatic Extracellular Matrix by Combined Methods of Immunohistochemistry, Proteomics and Scanning Electron Microscopy. *Curr. Res. Transl. Med.* **2017**, *65* (1), 31−39.
(90) Tian, C.; Clauser, K. R.; Öhlund, D.; Rickelt, S.; Huang, Y.; Gupta, M.; Mani, D. R.; Carr, S. A.; Tuveson, D. A.; Hynes, R. O. Proteomic Analyses of ECM during Pancreatic Ductal Adenocarcinoma Progression Reveal Different Contributions by Tumor and Stromal Cells. *Proc. Natl. Acad. Sci. U. S. A.* **2019**, *116* (39), 19609−19618.
(91) Lee, H. O.; Mullins, S. R.; Franco-Barraza, J.; Valianou, M.; Cukierman, E.; Cheng, J. D. FAP-Overexpressing Fibroblasts Produce an Extracellular Matrix That Enhances Invasive Velocity and Directionality of Pancreatic Cancer Cells. *BMC Cancer* **2011**, *11*, 11.
(92) Shi, Y.; Cang, L.; Zhang, X.; Cai, X.; Wang, X.; Ji, R.; Wang, M.; Hong, Y. The Use of Magnetic Resonance Elastography in Differentiating Autoimmune Pancreatitis from Pancreatic Ductal Adenocarcinoma: A Preliminary Study. *Eur. J. Radiol.* **2018**, *108* (36), 13−20.
(93) Xu, Y.; Cai, X.; Shi, Y.; Yin, M.; Lan, G.; Zhang, X.; Ji, R.; Chang Liu. Normative Pancreatic Stiffness Levels and Related Influences Established by Magnetic Resonance Elastography in Volunteers. *J. Magn. Reson. Imaging* **2020**, *52* (2), 448−458.
(94) Rice, A. J.; Cortes, E.; Lachowski, D.; Cheung, B. C. H.; Karim, S. A.; Morton, J. P.; Del Río Hernández, A. Matrix Stiffness Induces Epithelial-Mesenchymal Transition and Promotes Chemoresistance in Pancreatic Cancer Cells. *Oncogenesis* **2017**, *6* (7), 1−9.
(95) Itoh, Y.; Takehara, Y.; Kawase, T.; Terashima, K.; Ohkawa, Y.; Hirose, Y.; Koda, A.; Hyodo, N.; Ushio, T.; Hirai, Y.; Yoshizawa, N.; Yamashita, S.; Nasu, H.; Ohishi, N.; Sakahara, H. Feasibility of Magnetic Resonance Elastography for the Pancreas at 3T. *J. Magn. Reson. Imaging* **2016**, *43* (2), 384−390.
(96) Jafari, R.; Cramer, G. M.; Celli, J. P. Modulation of Extracellular Matrix Rigidity Via Riboflavin-Mediated Photocrosslinking Regulates Invasive Motility and Treatment Response in a 3D Pancreatic Tumor Model. *Photochem. Photobiol.* **2020**, *96* (2), 365−372.
(97) Lee, S. H.; Shim, K. Y.; Kim, B.; Sung, J. H. Hydrogel-Based Three-Dimensional Cell Culture for Organ-on-a-Chip Applications. *Biotechnol. Prog.* **2017**, *33* (3), 580−589.
(98) Zhao, Z.; Vizetto-Duarte, C.; Moay, Z. K.; Setyawati, M. I.; Rakshit, M.; Kathawala, M. H.; Ng, K. W. Composite Hydrogels in Three-Dimensional in Vitro Models. *Front. Bioeng. Biotechnol.* **2020**, *8* (June), 1−22.
(99) McKee, C. T.; Last, J. A.; Russell, P.; Murphy, C. J. Indentation versus Tensile Measurements of Young's Modulus for Soft Biological Tissues. *Tissue Eng., Part B* **2011**, *17* (3), 155−164.
(100) Czichy, C.; Spangenberg, J.; Günther, S.; Gelinsky, M.; Odenbach, S. Determination of the Young's Modulus for Alginate-Based Hydrogel with Magnetite-Particles Depending on Storage Conditions and Particle Concentration. *J. Magn. Magn. Mater.* **2020**, *501*, 166395.
(101) Fu, L.; Haage, A.; Kong, N.; Tanentzapf, G.; Li, H. Dynamic Protein Hydrogels with Reversibly Tunable Stiffness Regulate Human Lung Fibroblast Spreading Reversibly. *Chem. Commun.* **2019**, *55* (36), 5235−5238.
(102) Chen, R.; Xu, X.; Yu, D.; Xiao, C.; Liu, M.; Huang, J.; Mao, T.; Zheng, C.; Wang, Z.; Wu, X. Highly Stretchable and Fatigue Resistant Hydrogels with Low Young's Modulus as Transparent and Flexible Strain Sensors. *J. Mater. Chem. C* **2018**, *6* (41), 11193−11201.
(103) Nguyen, N. T.; Milani, A. H.; Jennings, J.; Adlam, D. J.; Freemont, A. J.; Hoyland, J. A.; Saunders, B. R. Highly Compressive and Stretchable Poly(Ethylene Glycol) Based Hydrogels Synthesised Using PH-Responsive Nanogels without Free-Radical Chemistry. *Nanoscale* **2019**, *11* (16), 7921−7930.
(104) Tirella, A.; Mattei, G.; La Marca, M.; Ahluwalia, A.; Tirelli, N. Functionalized Enzyme-Responsive Biomaterials to Model Tissue Stiffening in Vitro. *Front. Bioeng. Biotechnol.* **2020**, *8* (April), 1−14.
(105) Roa, J. J.; Oncins, G.; Diaz, J.; Sanz, F.; Segarra, M. Calculation of Young's Modulus Value by Means of AFM. *Recent Pat. Nanotechnol.* **2011**, *5*, 27−36.
(106) Suriano, R.; Zandrini, T.; De Marco, C.; Osellame, R.; Turri, S.; Bragheri, F. Nanomechanical Probing of Soft Matter through Hydrophobic AFM Tips Fabricated by Two-Photon Polymerization. *Nanotechnology* **2016**, *27* (15), 1.
(107) Galluzzi, M.; Biswas, C. S.; Wu, Y.; Wang, Q.; Du, B.; Stadler, F. J. Space-Resolved Quantitative Mechanical Measurements of Soft and Supersoft Materials by Atomic Force Microscopy. *NPG Asia Mater.* **2016**, *8* (11), No. e327.
(108) Markert, C. D.; Guo, X.; Skardal, A.; Wang, Z.; Bharadwaj, S.; Zhang, Y.; Bonin, K.; Guthold, M. Characterizing the Micro-Scale Elastic Modulus of Hydrogels for Use in Regenerative Medicine. *J. Mech. Behav. Biomed. Mater.* **2013**, *27*, 115−127.
(109) Akhtar, R.; Schwarzer, N.; Sherratt, M. J.; Watson, R. E. B.; Graham, H. K.; Trafford, A. W.; Mummery, P. M.; Derby, B. Nanoindentation of Histological Specimens. *J. Mater.* **2010**, *24* (3), 638−646.
(110) Kaufman, J. D.; Miller, G. J.; Morgan, E. F.; Klapperich, C. M. Time-Dependent Mechanical Characterization of Poly(2- Hydroxyethyl Methacrylate) Hydrogels Using Nanoindentation and Unconfined Compression. *J. Mater. Res.* **2008**, *23* (5), 1472−1481.
(111) Roether, J.; Bertels, S.; Oelschlaeger, C.; Bastmeyer, M.; Willenbacher, N. Microstructure, Local Viscoelasticity and Cell Culture Suitability of 3D Hybrid HA/Collagen Scaffolds. *PLoS One* **2018**, *13* (12), 10−12.
(112) Mattei, G.; Cacopardo, L.; Ahluwalia, A. Micro-Mechanical Viscoelastic Properties of Crosslinked Hydrogels Using the Nano-Epsilon Dot Method. *Materials* **2017**, *10* (8), 889.

https://dx.doi.org/10.1021/acsabm.0c01472
ACS Appl. Bio Mater. 2021, 4, 2233−2250

(113) Karavasili, C.; Tsongas, K.; Andreadis, I. I.; Andriotis, E. G.; Papachristou, E. T.; Papi, R. M.; Tzetzis, D.; Fatouros, D. G. Physico-Mechanical and Finite Element Analysis Evaluation of 3D Printable Alginate-Methylcellulose Inks for Wound Healing Applications. *Carbohydr. Polym.* **2020**, *247* (March), 116666.
(114) Picout, D. R.; Ross-Murphy, S. B. Rheology of Biopolymer Solutions and Gels. *Sci. World J.* **2003**, *3*, 105−121.
(115) Fung, Y. C. *Mechanical Properties of Living Tissues*; **1993**.
(116) Bilston, L. E. Soft Tissue Rheology and Its Implications for Elastography: Challenges and Opportunities. *NMR Biomed.* **2018**, *31* (10), 1−10.
(117) Abasalizadeh, F.; Moghaddam, S. V.; Alizadeh, E.; Akbari, E.; Kashani, E.; Fazljou, S. M. B.; Torbati, M.; Akbarzadeh, A.; Akbarzadeh, A. Alginate-Based Hydrogels as Drug Delivery Vehicles in Cancer Treatment and Their Applications in Wound Dressing and 3D Bioprinting (Journal of Biological Engineering. *J. Biol. Eng.* **2020**, *14* (1), 1−22.
(118) Axpe, E.; Oyen, M. L. Applications of Alginate-Based Bioinks in 3D Bioprinting. *Int. J. Mol. Sci.* **2016**, *17* (12), 1976.
(119) Skardal, A.; Atala, A. Biomaterials for Integration with 3-D Bioprinting. *Ann. Biomed. Eng.* **2015**, *43* (3), 730−746.
(120) Zhang, J.; Wehrle, E.; Vetsch, J. R.; Paul, G. R.; Rubert, M.; Müller, R. Alginate Dependent Changes of Physical Properties in 3D Bioprinted Cell-Laden Porous Scaffolds Affect Cell Viability and Cell Morphology. *Biomed. Mater.* **2019**, *14* (6), 65009.
(121) Giuseppe, M. Di; Law, N.; Webb, B.; A. Macrae, R.; Liew, L. J.; Sercombe, T. B.; Dilley, R. J.; Doyle, B. J. Mechanical Behaviour of Alginate-Gelatin Hydrogels for 3D Bioprinting. *J. Mech. Behav. Biomed. Mater.* **2018**, *79* (September 2017), 150−157.
(122) Liu, C.; Lewin Mejia, D.; Chiang, B.; Luker, K. E.; Luker, G. D. Hybrid Collagen Alginate Hydrogel as a Platform for 3D Tumor Spheroid Invasion. *Acta Biomater.* **2018**, *75*, 213−225.
(123) Fletcher, N. A.; Von Nieda, E. L.; Krebs, M. D. Cell-Interactive Alginate-Chitosan Biopolymer Systems with Tunable Mechanics and Antibody Release Rates. *Carbohydr. Polym.* **2017**, *175*, 765−772.
(124) Lueckgen, A.; Garske, D. S.; Ellinghaus, A.; Mooney, D. J.; Duda, G. N.; Cipitria, A. Enzymatically-Degradable Alginate Hydrogels Promote Cell Spreading and in Vivo Tissue Infiltration. *Biomaterials* **2019**, *217* (June), 119294.
(125) Ma, F.; Ge, Y.; Liu, N.; Pang, X.; Shen, X.; Tang, B. In Situ Fabrication of a Composite Hydrogel with Tunable Mechanical Properties for Cartilage Tissue Engineering. *J. Mater. Chem. B* **2019**, *7* (15), 2463−2473.
(126) Karvinen, J.; Joki, T.; Ylä-Outinen, L.; Koivisto, J. T.; Narkilahti, S.; Kellomäki, M. Soft Hydrazone Crosslinked Hyaluronan- and Alginate-Based Hydrogels as 3D Supportive Matrices for Human Pluripotent Stem Cell-Derived Neuronal Cells. *React. Funct. Polym.* **2018**, *124*, 29−39.
(127) Wang, Z.; Serban, B. A.; Serban, M. A. Recombinant Silk Fibroin Crystalline Regions as Biomaterial Alternatives to the Full-Length Protein. *ACS Biomater. Sci. Eng.* **2020**, *6* (12), 7004−7010.
(128) Vepari, C.; Kaplan, D. L. Silk as Biomaterial. *Prog. Polym. Sci.* **2012**, *100* (2), 130−134.
(129) Kapoor, S.; Kundu, S. C. Silk Protein-Based Hydrogels: Promising Advanced Materials for Biomedical Applications. *Acta Biomater.* **2016**, *31*, 17−32.
(130) Johari, N.; Moroni, L.; Samadikuchaksaraei, A. Tuning the Conformation and Mechanical Properties of Silk Fibroin Hydrogels. *Eur. Polym. J.* **2020**, *134*, 109842.
(131) Floren, M.; Bonani, W.; Dharmarajan, A.; Motta, A.; Migliaresi, C.; Tan, W. Human Mesenchymal Stem Cells Cultured on Silk Hydrogels with Variable Stiffness and Growth Factor Differentiate into Mature Smooth Muscle Cell Phenotype. *Acta Biomater.* **2016**, *31*, 156−166.
(132) Hasturk, O.; Jordan, K. E.; Choi, J.; Kaplan, D. L. Enzymatically Crosslinked Silk and Silk-Gelatin Hydrogels with Tunable Gelation Kinetics, Mechanical Properties and Bioactivity for Cell Culture and Encapsulation. *Biomaterials* **2020**, *232*, 119720.
(133) Sanz-Fraile, H.; Amoros, S.; Mendizabal, I.; Galvez-Monton, C.; Prat-Vidal, C.; Bayes-Genis, A.; Navajas, D.; Farre, R.; Otero, J. *Tissue Eng., Part A* **2020**, *26*, 358.
(134) Khoo, A. S.; Valentin, T. M.; Leggett, S. E.; Bhaskar, D.; Bye, E. M.; Benmelech, S.; Ip, B. C.; Wong, I. Y. Breast Cancer Cells Transition from Mesenchymal to Amoeboid Migration in Tunable Three-Dimensional Silk-Collagen Hydrogels. *ACS Biomater. Sci. Eng.* **2019**, *5* (9), 4341−4354.
(135) Buitrago, J. O.; Patel, K. D.; El-Fiqi, A.; Lee, J. H.; Kundu, B.; Lee, H. H.; Kim, H. W. Silk Fibroin/Collagen Protein Hybrid Cell-Encapsulating Hydrogels with Tunable Gelation and Improved Physical and Biological Properties. *Acta Biomater.* **2018**, *69*, 218−233.
(136) Lu, X.; Ding, Z.; Xu, F.; Lu, Q.; Kaplan, D. L. Subtle Regulation of Scaffold Stiffness for the Optimized Control of Cell Behavior. *ACS Appl. Bio Mater.* **2019**, *2* (7), 3108−3119.
(137) Xiao, L.; Liu, S.; Yao, D.; Ding, Z.; Fan, Z.; Lu, Q.; Kaplan, D. L. Fabrication of Silk Scaffolds with Nanomicroscaled Structures and Tunable Stiffness. *Biomacromolecules* **2017**, *18* (7), 2073−2079.
(138) Wang, X.; Ding, Z.; Wang, C.; Chen, X.; Xu, H.; Lu, Q.; Kaplan, D. L. Bioactive Silk Hydrogels with Tunable Mechanical Properties. *J. Mater. Chem. B* **2018**, *6* (18), 2739−2746.
(139) Liu, J.; Ding, Z.; Lu, G.; Wang, J.; Wang, L.; Lu, Q. Amorphous Silk Fibroin Nanofiber Hydrogels with Enhanced Mechanical Properties. *Macromol. Biosci.* **2019**, *19* (12), 1900326.
(140) Van Den Bulcke, A. I.; Bogdanov, B.; De Rooze, N.; Schacht, E. H.; Cornelissen, M.; Berghmans, H. Structural and Rheological Properties of Methacrylamide Modified Gelatin Hydrogels. *Biomacromolecules* **2000**, *1* (1), 31−38.
(141) Nichol, J. W.; Koshy, S. T.; Bae, H.; Hwang, C. M.; Yamanlar, S.; Khademhosseini, A. Cell-Laden Microengineered Gelatin Methacrylate Hydrogels. *Biomaterials* **2010**, *31* (21), 5536−5544.
(142) Ha, M.; Athirasala, A.; Tahayeri, A.; Menezes, P. P.; Bertassoni, L. E. Micropatterned Hydrogels and Cell Alignment Enhance the Odontogenic Potential of Stem Cells from Apical Papilla In-Vitro. *Dent. Mater.* **2020**, *36* (1), 88−96.
(143) Engler, A. J.; Sen, S.; Sweeney, H. L.; Discher, D. E. Matrix Elasticity Directs Stem Cell Lineage Specification. *Cell* **2006**, *126* (4), 677−689.
(144) Lin, C. H.; Su, J. J. M.; Lee, S. Y.; Lin, Y. M. Stiffness Modification of Photopolymerizable Gelatin-Methacrylate Hydrogels Influences Endothelial Differentiation of Human Mesenchymal Stem Cells. *J. Tissue Eng. Regener. Med.* **2018**, *12* (10), 2099−2111.
(145) Wu, Y.; Xiang, Y.; Fang, J.; Li, X.; Lin, Z.; Dai, G.; Yin, J.; Wei, P.; Zhang, D. The Influence of the Stiffness of GelMA Substrate on the Outgrowth of PC12 Cells. *Biosci. Rep.* **2019**, *39* (1), 1−9.
(146) Kim, C.; Young, J. L.; Holle, A. W.; Jeong, K.; Major, L. G.; Jeong, J. H.; Aman, Z. M.; Han, D. W.; Hwang, Y.; Spatz, J. P.; Choi, Y. S. Stem Cell Mechanosensation on Gelatin Methacryloyl (GelMA) Stiffness Gradient Hydrogels. *Ann. Biomed. Eng.* **2020**, *48* (2), 893−902.
(147) Jiang, T.; Zhao, J.; Yu, S.; Mao, Z.; Gao, C.; Zhu, Y.; Mao, C.; Zheng, L. Untangling the Response of Bone Tumor Cells and Bone Forming Cells to Matrix Stiffness and Adhesion Ligand Density by Means of Hydrogels. *Biomaterials* **2019**, *188* (October 2018), 130−143.
(148) Zhan, X. Effect of Matrix Stiffness and Adhesion Ligand Density on Chondrogenic Differentiation of Mesenchymal Stem Cells. *J. Biomed. Mater. Res., Part A* **2020**, *108* (3), 675−683.
(149) Peter, M.; Singh, A.; Mohankumar, K.; Jeenger, R.; Joge, P. A.; Gatne, M. M.; Tayalia, P. Gelatin-Based Matrices as a Tunable Platform to Study in Vitro and in Vivo 3D Cell Invasion. *ACS Appl. Bio Mater.* **2019**, *2* (2), 916−929.
(150) Xiao, W.; Tan, Y.; Li, J.; Gu, C. F.; Li, H.; Li, B.; Liao, X. Fabrication and Characterization of Silk Microfiber-Reinforced Methacrylated Gelatin Hydrogel with Turnable Properties. *J. Biomater. Sci., Polym. Ed.* **2018**, *29* (17), 2068−2082.
(151) Collins, M. N.; Birkinshaw, C. Hyaluronic Acid Based Scaffolds for Tissue Engineering - A Review. *Carbohydr. Polym.* **2013**, *92* (2), 1262−1279.

https://dx.doi.org/10.1021/acsabm.0c01472
ACS Appl. Bio Mater. 2021, 4, 2233−2250

(152) Asim, M. H.; Silberhumer, S.; Shahzadi, I.; Jalil, A.; Matuszczak, B.; Bernkop-Schnürch, A. S-Protected Thiolated Hyaluronic Acid: In-Situ Crosslinking Hydrogels for 3D Cell Culture Scaffold. *Carbohydr. Polym.* **2020**, *237* (March), 116092.
(153) Aviv, M.; Halperin-Sternfeld, M.; Grigoriants, I.; Buzhansky, L.; Mironi-Harpaz, I.; Seliktar, D.; Einav, S.; Nevo, Z.; Adler-Abramovich, L. Improving the Mechanical Rigidity of Hyaluronic Acid by Integration of a Supramolecular Peptide Matrix. *ACS Appl. Mater. Interfaces* **2018**, *10* (49), 41883−41891.
(154) Ekerdt, B. L.; Fuentes, C. M.; Lei, Y.; Adil, M. M.; Ramasubramanian, A.; Segalman, R. A.; Schaffer, D. V. Thermoreversible Hyaluronic Acid-PNIPAAm Hydrogel Systems for 3D Stem Cell Culture. *Adv. Healthc. Mater.* **2018**, *7* (12), 1−12.
(155) Kuss, M.; Kim, J.; Qi, D.; Wu, S.; Lei, Y.; Chung, S.; Duan, B. Effects of Tunable, 3D-Bioprinted Hydrogels on Human Brown Adipocyte Behavior and Metabolic Function. *Acta Biomater.* **2018**, *71*, 486−495.
(156) Duan, Y.; Li, X.; Zuo, X.; Shen, T.; Yu, S.; Deng, L.; Gao, C. Migration of Endothelial Cells and Mesenchymal Stem Cells into Hyaluronic Acid Hydrogels with Different Moduli under Induction of Pro-Inflammatory Macrophages. *J. Mater. Chem. B* **2019**, *7* (36), 5478−5489.
(157) Narkhede, A. A.; Crenshaw, J. H.; Manning, R. M.; Rao, S. S. The Influence of Matrix Stiffness on the Behavior of Brain Metastatic Breast Cancer Cells in a Biomimetic Hyaluronic Acid Hydrogel Platform. *J. Biomed. Mater. Res., Part A* **2018**, *106* (7), 1832−1841.
(158) Bonnescœur, S.; Morin-Grognet, S.; Thoumire, O.; Le Cerf, D.; Boyer, O.; Vannier, J. P.; Labat, B. Hyaluronan-Based Hydrogels as Versatile Tumor-like Models: Tunable ECM and Stiffness with Genipin-Crosslinking. *J. Biomed. Mater. Res., Part A* **2020**, *108* (5), 1256−1268.
(159) Xiao, W.; Zhang, R.; Sohrabi, A.; Ehsanipour, A.; Sun, S.; Liang, J.; Walthers, C. M.; Ta, L.; Nathanson, D. A.; Seidlits, S. K. Brain-Mimetic 3D Culture Platforms Allow Investigation of Cooperative Effects of Extracellular Matrix Features on Therapeutic Resistance in Glioblastoma. *Cancer Res.* **2018**, *78* (5), 1358−1370.
(160) Li, J.; Xing, R.; Bai, S.; Yan, X. Recent Advances of Self-Assembling Peptide-Based Hydrogels for Biomedical Applications. *Soft Matter* **2019**, *15* (8), 1704−1715.
(161) Bairagi, D.; Biswas, P.; Basu, K.; Hazra, S.; Hermida-Merino, D.; Sinha, D. K.; Hamley, I. W.; Banerjee, A. Self-Assembling Peptide-Based Hydrogel: Regulation of Mechanical Stiffness and Thermal Stability and 3D Cell Culture of Fibroblasts. *ACS Appl. Bio Mater.* **2019**, *2* (12), 5235−5244.
(162) Jian, H.; Wang, M.; Dong, Q.; Li, J.; Wang, A.; Li, X.; Ren, P.; Bai, S. Dipeptide Self-Assembled Hydrogels with Tunable Mechanical Properties and Degradability for 3D Bioprinting. *ACS Appl. Mater. Interfaces* **2019**, *11* (50), 46419−46426.
(163) Sheikholeslam, M.; Wheeler, S. D.; Duke, K. G.; Marsden, M.; Pritzker, M.; Chen, P. Peptide and Peptide-Carbon Nanotube Hydrogels as Scaffolds for Tissue & 3D Tumor Engineering. *Acta Biomater.* **2018**, *69*, 107−119.
(164) Ichise, S. F.; Takeuchi, S.; Aoki, S.; Kuroda, K. C.; Nose, H.; Masuda, R.; Koide, T. Development of a Collagen-like Peptide Polymer via End-to-End Disulfide Cross-Linking and Its Application as a Biomaterial. *Acta Biomater.* **2019**, *94*, 361−371.
(165) Zhang, X.; Wang, C. Supramolecular Amphiphiles. *Chem. Soc. Rev.* **2011**, *40* (1), 94−101.
(166) Redondo-Gómez, C.; Abdouni, Y.; Becer, C. R.; Mata, A. Self-Assembling Hydrogels Based on a Complementary Host-Guest Peptide Amphiphile Pair. *Biomacromolecules* **2019**, *20* (6), 2276−2285.
(167) Zhu, J. Bioactive Modification of Poly(Ethylene Glycol) Hydrogels for Tissue Engineering. *Biomaterials* **2010**, *31* (17), 4639−4656.
(168) Crocini, C.; Walker, C. J.; Anseth, K. S.; Leinwand, L. A. Three-Dimensional Encapsulation of Adult Mouse Cardiomyocytes in Hydrogels with Tunable Stiffness. *Prog. Biophys. Mol. Biol.* **2020**, *154* (xxxx), 71−79.
(169) Shih, H.; Lin, C. C. Tuning Stiffness of Cell-Laden Hydrogel: Via Host-Guest Interactions. *J. Mater. Chem. B* **2016**, *4* (29), 4969−4974.
(170) Hiemstra, C.; Van Der Aa, L. J.; Zhong, Z.; Dijkstra, P. J.; Feijen, J. Novel in Situ Forming, Degradable Dextran Hydrogels by Michael Addition Chemistry: Synthesis, Rheology, and Degradation. *Macromolecules* **2007**, *40* (4), 1165−1173.
(171) Massia, S. P.; Stark, J. Immobilized RGD Peptides on Surface-Grafted Dextran Promote Biospecific Cell Attachment. *J. Biomed. Mater. Res.* **2001**, *56* (3), 390−399.
(172) Liu, Y.; Chan-Park, M. B. A Biomimetic Hydrogel Based on Methacrylated Dextran-Graft-Lysine and Gelatin for 3D Smooth Muscle Cell Culture. *Biomaterials* **2010**, *31* (6), 1158−1170.
(173) Kim, S.; Park, M. R.; Choi, C.; Kim, J. B.; Cha, C. Synergistic Control of Mechanics and Microarchitecture of 3D Bioactive Hydrogel Platform to Promote the Regenerative Potential of Engineered Hepatic Tissue. *Biomaterials* **2021**, *270*, 120688.
(174) Davidson, C. D.; Jayco, D. K. P.; Matera, D. L.; DePalma, S. J.; Hiraki, H. L.; Wang, W. Y.; Baker, B. M. Myofibroblast Activation in Synthetic Fibrous Matrices Composed of Dextran Vinyl Sulfone. *Acta Biomater.* **2020**, *105*, 78−86.

https://dx.doi.org/10.1021/acsabm.0c01472
ACS Appl. Bio Mater. 2021, 4, 2233−2250